R. & M. No. 3487

MINISTRY OF AVIATION

AERONAUTICAL RESEARCH COUNCIL
REPORTS AND MEMORANDA

The Calculation of the Spanwise Loading of Sweptback Wings with Flaps or All-Moving Tips at Subsonic Speeds

by

G. G. Brebner, M.A. and D. A. Lemaire, B.Mech.E.

LONDON: HER MAJESTY'S STATIONERY OFFICE
1967
PRICE 17*s.* 0*d.* NET

The Calculation of the Spanwise Loading of Sweptback Wings with Flaps or All-Moving Tips at Subsonic Speeds

by

G. G. Brebner, M.A. and D. A. Lemaire, B.Mech.E.

COMMUNICATED BY THE DEPUTY CONTROLLER AIRCRAFT (RESEARCH AND DEVELOPMENT), MINISTRY OF AVIATION

Reports and Memoranda No. 3487*
September, 1955

Summary.

The results of some electric tank tests by Duquenne and Grandjean[8] on wings of 45 deg sweepback with trailing edge flaps have been analysed to provide the basis for a method of calculating the spanwise loading. The analysis yielded information about the effect of sweep on the equivalent incidence of a section with flap, on the downwash factor and on the spanwise loading distribution with an incidence discontinuity. Interpolation formulae are developed to extend the results to wings of any sweep and flap span, and thus a complete calculation method is presented for the spanwise loading with this type of control.

The calculation method is tentatively extended to a wing with all-moving tip control, and the results compared with those of Thomas and Mangler[13]. There is a marked discrepancy between the two calculations. Further electric tank tests to fill this, and other gaps are suggested.

LIST OF CONTENTS

* Replaces R.A.E. Report Aero 2553—A.R.C. 18 273.

LIST OF APPENDICES

LIST OF TABLES

LIST OF ILLUSTRATIONS

---

1. *Introduction.*

Many investigations have been made into the load distribution on plane swept wings, but comparatively few have dealt with the case of deflected flaps or ailerons. Some important flight conditions are associated with this configuration and it is therefore desirable to have a simple and reliable method for calculating the loading on swept wings with flaps. The load distribution is also required to determine aero-elastic effects, such as aileron reversal. The boundary layer may have a big effect on flap efficiency but this cannot be determined from experiments unless the inviscid flap efficiency is known.

Two main difficulties are apparent in a theoretical treatment of this problem. Firstly, a deflected hinged flap changes the chordwise loading and hence some of the sectional characteristics of the aerofoil. Secondly, there is, in effect, a discontinuous change of incidence at some spanwise position. In the case of an unswept wing of comparatively large aspect ratio the following procedure appears to be generally accepted as a sufficiently accurate solution of the spanwise loading due to flap deflection. The sectional characteristics are taken from Glauert's theory[1] (or, more accurately, Keune's treatment[2,3]) for a thin, kinked two-dimensional plate. Theoretical or empirical corrections to take account of aerofoil thickness, gap, etc., can be applied. Thus values for the 'equivalent incidence', $\Delta\alpha$ (which is equal in magnitude but opposite in sign to the zero lift angle) due to flap deflection are obtained, as well as the pitching moment at zero lift. Within the assumptions of linearised theory the sectional lift slope is left unaltered, as is the slope of the pitching moment vs. lift curve. Using Prandtl's classical aerofoil equation, $\Delta\alpha$ is a twist term which has a non-zero value at sections with deflected flap, and is zero elsewhere. A sufficiently accurate solution of the aerofoil equation for such a discontinuous incidence distribution can be obtained by Multhopp's method[4], in which the discontinuity is split off and the loading calculated in two parts.

Turning now to swept wings, one class of method typified by that of DeYoung[16,17], applies the 'three-quarter chord theorem' (valid only for unswept two-dimensional wings without flaps) in conditions far beyond the limits of its validity: i.e., the loading is concentrated on the quarter-chord line and the boundary conditions, involving the velocities induced by the trailing vortices as well as the bound vortices, are satisfied on the three-quarter chord line. In Refs. 16 and 17 these boundary conditions for wings with flaps are artificially modified on the basis of the spanwise loading as the aspect ratio tends to zero. The boundary conditions do not take account of centre and tip effects on swept wings and are satisfied at only four spanwise stations on a half-wing. This method offers little hope of understanding the flow processes on swept wings with flaps, and the adequacy of the results is questionable.

Another class of method for calculating the spanwise loading of a three-dimensional wing treats the double downwash integral as a whole, over the wing surface and the wake, and fulfils the boundary

condition (i.e., the correct slope of the given wing) at a number of chordwise and spanwise positions. For example, in Multhopp's recent method[5] two chordwise and fifteen spanwise points are normally used, i.e. a total of 30 pivotal points. The computing time required is roughly proportional to the square of the number of points and it is not practicable to choose more than about three chordwise points. To make the best possible use of this limited number an attempt is made to choose their positions so that the sectional properties are obtained most accurately. For example, with two chordwise points on a wing without flaps, two coefficients, say the lift and the pitching moment, can be used to find the optimum positions of the points. The flaw in this procedure is that two-dimensional theoretical chordwise load distributions are used as the basis for the calculation of the optimum positions, and this is certainly not valid for a general section on a swept wing. It can easily be shown that, using chord-wise loadings known to be more applicable to swept wings (e.g. from Ref. 6), quite different positions for the chordwise points are obtained. Thus it is really necessary to know the answers one is looking for before one can place the chordwise pivotal points to best advantage.

In the case of a swept wing with flaps the chordwise points are determined as above. The local incidences are obtained by using two-dimensional flap theory which again is certainly not valid for swept wings, and the same objections apply as in the case of the wing without flaps, only more strongly.

If the method yielded information about the chordwise loading it might be possible to arrive at a valid estimate of this loading—and hence of the optimum points—by successive approximation. But two or three chordwise points cannot supply the basic information and this procedure is impossible.

Another drawback of this kind of method is that the spanwise incidence discontinuity at the edge of the flap cannot be treated as such. Instead, an approximate fairing process must be employed. This means that a large number of spanwise pivotal points is desirable but the computing effort involved in 31 points (the next highest number after 15) is much greater.

It therefore seems reasonable to conclude that methods like that of Ref. 5 depend for their accuracy on the appropriate choice of the very limited number of chordwise pivotal points, and that this choice cannot be made on any valid grounds for a three-dimensional wing without enough fore-knowledge to make the calculation superfluous anyway. The alternative is to allow a large number of chordwise points arbitrarily spaced over the chord. This is beyond the possibilities of numerical computation by such methods.

It is not, however, beyond the capabilities of an analogue computer and the three-dimensional electrolytic tank offers an excellent prospect of obtaining solutions of the spanwise and chordwise loadings of three-dimensional wings, including wings with flaps. Such tank results provide, in fact, a numerical solution of Laplace's equation, with the same boundary conditions as in linearized theory. Since the number of chordwise pivotal points can be significantly greater than is possible in practice with any of the so-called 'lifting-surface' methods, the accuracy obtainable is also considerably increased and the electrolytic tank appears to be the most powerful method available for the solution of such problems. It is not really suitable for routine calculations, however, owing to the need for constructing, in effect, a different model for each planform. We therefore consider a third class of calculation method as a basis for a routine procedure.

This class of method for swept wings is exemplified by Ref. 6. The downwash integral over the wing is treated in two parts, and thus the concept of an induced incidence from the streamwise vortices is retained. Using Ref. 6 as a framework a simple method of calculating the spanwise loading of swept wings with flaps can be devised provided certain data are available. The main features of this approach are:

(i) The assumptions and approximations of linearized theory are retained, including the principle of superposition of incidence, camber and flap contributions to the lift.

(ii) At any spanwise position the effect of the induced incidence due to the streamwise vortices may be represented by a mean induced incidence over the chord, but the values appropriate to a plane or cambered wing are no longer valid.

(iii) The sectional lift slope is independent of the section shape.

(iv) The representation of the flap effect as an equivalent incidence, $\Delta\alpha$, is retained, but the two-dimensional values (e.g. Glauert[1], Keune[2, 3]) are no longer valid in general.

(v) The spanwise discontinuity of equivalent incidence at the edge of the flap can be treated by splitting off the discontinuity in the manner of Multhopp[4].

(vi) Corrections, empirical or otherwise, can be simply applied to sectional properties such as $\Delta\alpha$ to allow for the effects of wing thickness, viscosity, etc.

In item (ii) above it is not possible to calculate theoretical values of the mean induced incidence owing to the complicated nature of the streamwise vortex patterns. Regarding item (iv), the application of the method of Ref. 6 to cambered sections[7] indicated that the sectional equivalent incidence and pitching moment on a swept wing varied with angle of sweep and spanwise position, and the same may be expected to be true of a kinked flap section. A theoretical investigation has confirmed this and will be published separately, but no theoretical explanation is attempted here.

Instead, the results of some systematic tests in a three-dimensional electrolytic tank have been analysed on the basis of the method outlined above to provide numerical data on $\Delta\alpha$ and on the values of the mean induced incidence which is closely bound up with the spanwise loading functions associated with the incidence discontinuity. These tests were conducted by Duquenne and Grandjean[8] in the electrolytic tank of Professor Malavard[9], and the results were kindly put at our disposal. They consist of measurements of spanwise and chordwise loadings on a constant chord wing of 45 deg sweepback, with various flap configurations. The $\Delta\alpha$ distributions to produce such spanwise loadings have been calculated, and by expressing the results in terms of the parameter n (*see* Ref. 6) which combines sweep and spanwise effects it is possible to apply these results for $\Delta\alpha$ to wings of different sweepback. Also the spanwise loading functions can be interpolated to apply to wings with different flap sizes and sweep angles. This makes unnecessary the testing of many wing planforms in the electrolytic tank.

Thus the accuracy attributed earlier to electrolytic tank solutions of wing loading problems has been used to provide data for a routine calculation method for sweptback wings with flaps. The main conclusion of the present report is that this procedure is successful and that the accuracy is adequate for most purposes. There seems to be no need for any significant refinements in the framework of the analysis (i.e. the theory of Ref. 6). However, electrolytic tank tests of similar configuration employing 8 and 11 chordwise points have shown noticeable differences in the measured spanwise loadings, and it may be that even 11 points is not enough, especially near the centre and tip sections where sectional properties are changing rapidly. This emphasises the unreliability of methods which are limited to only 2 or 3 chordwise points. Further tank results to fill gaps in the data are desirable.

The present theory will find a useful application in the problem of boundary-layer control over deflected flaps, either by injecting or sucking air at the hinge position. If the flow does not separate at the flap the conditions of inviscid flow are approached. Injection and suction could be used to improve some undesirable features of sweptback wings, for instance by making the spanwise distribution of lift or minimum pressure more uniform. In designing for such purposes experimental results for two-dimensional aerofoils cannot be directly applied to swept wings, as the results of the present note show. The flap-chord ratio, the flap span and deflection and the rate of injection or suction must depend on the angle of sweep and must be suitably graded over the span. The present theory may help in such design. If the spanwise loading is altered the induced drag will also be changed, perhaps for the worse. For example, on sweptback wings a uniform spanwise C_L distribution does not lead to minimum induced drag (*see* Ref. 18). The present theory covers the calculation of the induced drag in any particular case.

Although the electrolytic tank is a form of analogue computer, results obtained on it will usually be described in the text as 'tests' in order to differentiate them from calculations by the routine method. The investigations apply to inviscid, incompressible flow. An extension to compressible flow at subcritical Mach numbers can be made by applying the Prandtl-Glauert analogy[6].

In the following pages Sections 2 and 3 contain a qualitative theoretical discussion : Section 4 contains the details of the configurations tested and Section 5 the method of analysis. The results for the equivalent incidence and spanwise loading functions are discussed in Sections 6 and 7, and formulae for extending the results to other planforms are given in Section 8. The suggested calculation method is summarized in Section 9 (which may be read by itself). Section 10 deals with an allied problem involving all-moving tip controls, and the concluding discussion is given in Section 11.

2. *The Downwash Factor, ω*

In linearized aerofoil theory the downwash at any spanwise position on a wing due to the trailing vortices may be expressed as $\omega \times$ half the downwash at the same spanwise position at infinity downstream: i.e., $\alpha_i = \omega \times \alpha_{i0}$. ω is called the downwash factor, and this section deals with its behaviour in the case of wings—especially swept wings—with flaps, so that the subsequent analysis of experimental data may have a sound basis. ω varies with sweep and aspect ratio. For a plane unswept wing, $\omega \to 1$ as A, the aspect ratio, $\to \infty$, and $\omega \to 2$ as $A \to 0$. For a plane swept wing, the same limits can be accepted, but the variation of ω between the limits is different from the case of an unswept wing. Küchemann[6] has developed formulae for ω which give good agreement with experiment both for swept and unswept wings. To investigate the value of ω on wings with flaps let us return to some elementary notions.

2.1 *Isolated Trailing Vortices*

The results of this section were established many years ago in connection with Munk's stagger theorem. They are repeated here from the point of view of the downwash on swept wings. Consider a single line vortex in the free stream direction originating at a point on an unswept wing and extending to infinity downstream, the chordwise ordinate of the point of origin being x_v (x,y are non-dimensional with the chord: i.e. $x = 0$ at the leading edge and 1 at the trailing edge). In the terminology of Ref. 6 this vortex is a 'chordwise' or 'streamwise' vortex on the wing and a 'trailing' vortex in the wake. For the sake of simplicity such vortices will here be referred to as trailing vortices even though they extend over part of the chord. Fig. 1 shows the wing and the vortex AB.

In Appendix I an expression is derived for the mean downwash over the chord at stations on either side of the trailing vortex. This mean downwash is greater than α_{i0} if $0 \leqslant x_v < 0{\cdot}5$, i.e., the unswept downwash factor $\omega_1 > 1$. At $x_v = 0{\cdot}5$, $\omega_1 = 1$ and for $0{\cdot}5 < x_v \leqslant 1{\cdot}0$, $\omega_1 < 1$. As the distance from the vortex increases $\omega_1 \to 1$ for all values of x_v. The variation of ω_1 with the distance from the vortex, $y - y_v$, is shown in Fig. 2 for values uf x_v between 0 and 1.

If we now consider a single trailing vortex originating at a chordwise position x_v on a sweptback wing, the results of Appendix I show that the mean downwash over the chord at a section inboard of the vortex is less than it would be at the same section of the corresponding unswept wing (*see* Fig. 1). This ratio,

$$\begin{pmatrix}\text{mean downwash over chord}\\ \text{of swept wing}\end{pmatrix} \div \begin{pmatrix}\text{mean downwash over chord}\\ \text{of unswept wing}\end{pmatrix}$$

is called ω_2, so that the complete downwash factor, ω, for the single vortex on the swept wing is $\omega = \omega_1 \times \omega_2$. Near the vortex on the inboard side ω_2 decreases as x_v increases. For all values of x_v ω_2 decreases monotonically as the distance of the section inboard of the vortex increases and tends to a limit as this distance tends to infinity. This limit, the same for all values of x_v, is $1 - \sin\varphi$ where φ is the angle of sweep. Outboard of the vortex the mean downwash over the chord is greater than on the corresponding unswept wing, and $\omega_2 > 1$. ω_2 increases as x_v increases and tends to a limit (but not so quickly as inboard and not necessarily monotonically) as the distance from the vortex tends to infinity. This limit is $1 + \sin\varphi$. The spanwise variation of ω_2 inboard and outboard of the vortex is shown in Fig. 3 for values of x_v between 0 and 1. ω_2 has its maximum value less than one chord from the vortex for $0{\cdot}5 < x_v \leqslant 1{\cdot}0$. It may be noted that $\omega_1 \to 1$ as $y \to \infty$ and $\omega_2 \to 1$ as $y \to 0$.

2.2. *Wings Without flaps.*

In the light of the above results, consider the downwash induced by the trailing vortices on swept and unswept wings without flaps. The problem is extremely difficult quantitatively, since there are now chordwise and spanwise distributions of vorticity instead of isolated vortices. However, a qualitative discussion is possible on the basis that the trailing vortex strength is much greater at the tips than anywhere else on the wing. It is also necessary to assume a value for x_v based on the chordwise vortex distribution. The local centre of pressure is a suitable approximation. This means that on all wings with symmetrical or conventionally cambered sections $0 \leqslant x_v \leqslant 0{\cdot}5$. In the classical linearized theory of thin

unswept aerofoils of high aspect ratio the downwash over the wing was assumed to be half that at infinity downstream, i.e., $\omega_1 = 1$. Fig. 2 shows that this is justifiable for most parts of a high aspect-ratio wing, whatever the value of x_v, assuming that the trailing vortex from the tip is the chief contributor to the downwash. As the aspect ratio decreases the factor ω_1 increases to a value appreciably greater than 1. In the theory of wings of low aspect ratio ω_1 is regarded as tending to 2 as $A \to 0$. This is justifiable, since at $A = 0$ the lift would be concentrated at the leading edge, and $x_v = 0$. Thus the limit $\omega_1 = 2$ is consistent with Fig. 2. As A increases above zero the centre of pressure moves back and x_v increases, so that no single curve of Fig. 2 represents the variation of ω_1 with A. Küchemann[6] introduced the following formula for ω on unswept wings :—

$$\omega = 2 - \frac{1}{\left\{1 + \left(\frac{a_0}{\pi A}\right)^2\right\}^{\frac{1}{4}}} \tag{1}$$

where a_0 is the two-dimensional lift slope. This is plotted in Fig. 2 and shows the effect of varying centre of pressure.

Turning now to swept wings, the downwash factor due to sweep, ω_2, must be taken into account, the complete factor for a single trailing vortex being $\omega = \omega_1 \times \omega_2$. If we consider the main effect to be due to the strong tip vortex, then clearly ω is less for a sweptback wing than an unswept wing of the same aspect ratio, since $\omega_2 < 1$. However, there are three effects of sweepback which tend to oppose this decrease in ω:

(i) The centre of pressure near the tip of a sweptback wing is further forward than at the tip of an unswept wing, hence x_v is smaller and ω_1 and ω_2 are both increased.

(ii) The characteristic spanwise loading of a sweptback wing has a 'dip' in the middle and hence the trailing vortices near the centre of the wing induce a downwash outboard and an upwash inboard, the former covering most of the wing.

(iii) The downwash factor ω_2' associated with a trailing vortex from the opposite half-wing is greater than ω_2 associated with the corresponding vortex on the first side. This can be seen from Fig. 1, $A'B'$ being the vortex from the opposite half-wing. (Its effect is more easily calculated with respect to the infinite swept wing shown dotted.) The effect of vortices from the opposite half-wing is usually fairly small.

These three factors therefore tend to counteract the sweep effect of the tip vortex and experimental evidence has shown that the downwash factor ω is only slightly less for a sweptback wing than for an unswept wing. Küchemann's formula for swept wings,[6]

$$\omega = 2 - \frac{1}{1 + \left\{\frac{a_0 \cos\phi}{\pi A}\right\}^{2 \; \frac{1}{4(1+|\varphi|/\frac{1}{2}\pi)}}} \tag{2}$$

takes account of this fact. As an example, for an unswept thin wing of aspect ratio 4, the Küchemann formula gives $\omega = 1{\cdot}054$: for a corresponding wing with 45 deg sweepback, $\omega = 1.022$.

Similar considerations in the opposite sense apply to swept-forward wings, so that the resultant downwash factor is slightly greater than for the corresponding unswept wing.

In the above cases of swept and unswept wings the value of ω is regarded as constant over the whole span. This is clearly not so, but the error is only appreciable near the tips where the loading is approaching zero, and hence the final error in any loading calculation is not great.

2.3. *Unswept Wings with Deflected flaps.*

Section 2.2 dealt with cases where the centre of pressure is fairly far forward on the chord, such as a plane or conventionally cambered wing at incidence. We will now consider cases where the centre of pressure is further back, in particular wings with deflected trailing edge flaps. On such wings the local

c.p. at a section with flap may be at $x = 0{\cdot}5$ or more, most of the local lift force being in the neighbourhood of the hinge. Thus the variation of ω with A appropriate to a plane wing may not be applicable to a wing with flap.

Consider first an unswept wing at zero incidence with full span trailing-edge flap deflected. Since there is no sweep $\omega_2 = 1$ and the only relevant factor is ω_1. The spanwise loading will be similar to that of a plane wing at incidence, since the lifting effect of the flap is, to a good approximation, the same at all points along the span. If we take x_v of the tip vortex as the local centre of pressure, then ω_1 increases as A decreases for $0 \leqslant x_v < 0{\cdot}5$ and ω_1 decreases as A decreases for $0{\cdot}5 < x_v \leqslant 1{\cdot}0$. Electrolytic tank tests have shown that for a trailing-edge flap of conventional chord ratio the c.p. is in fact at about 0·5 chord.* Thus there is likely to be little effect of aspect ratio on ω in such a case: i.e., $\omega = 1$ always. In this connection it is interesting to consider the theory of R. T. Jones[15] for wings of very small A, with the aim of obtaining a rough estimate of the mean value of the downwash factor ω from these concepts. Although this theory is developed for pointed wings the sweep is of no significance in the limit $A \to 0$. For such a wing $\bar{C}_L = \pi/2.A.\alpha$. The incidence α is equal to that induced by the streamwise vortices, α_i, since $\alpha_e \to 0$ as $A \to 0$. Also $\omega \to 2$ as $A \to 0$ so that $\alpha_i = 2\alpha_{i0}$. If the wing is at zero incidence but has a full-span trailing-edge flap with $x_v = 0{\cdot}5$ and β, the flap deflection, constant over the span, all the lift force is concentrated in the area of the flap which is 0·5 that of the whole wing. Thus the aspect ratio of the flap is $A_F = 2A$ and the lift coefficient based on the whole wing is

$$\bar{C}_L = \frac{1}{2}.\frac{\pi}{2}.2A.\beta$$

$$= \frac{\pi}{2}.A.\beta$$

Since the flow in planes $x =$ constant may be considered two-dimensional as $A \to 0$ the equivalent incidence $\Delta\alpha = 0{\cdot}5\ \beta$. Working out C_L on the basis of the whole wing at incidence $\Delta\alpha$,

$$\bar{C}_L = \frac{\pi}{2} \quad \frac{\beta}{2}$$

i.e., half the previous value. This indicates that in the second calculation ω (which is based on the mean downwash) should be taken equal to 1, which is reasonable on the simple physical grounds of the length of the streamwise vortices (the lift being concentrated at the hinge). Thus for a half-chord flap, $\omega = 1$ over the whole aspect-ratio range. In the general case of a hinge at $x = x_H$, the limit of ω as $A \to 0$ should be $\omega \to 2(1 - x_H)$, as in Fig. 2.

If we now consider a similar unswept wing with part-span flap extending outwards from the centre section, there is a strong trailing vorticity from the position of discontinuity at the outer end of the flap and more from the tip. Outboard of the flap the c.p. is further forward than $x = 0{\cdot}5$ and so ω_1 appropriate to the tip vortex $\geqslant 1$. At the discontinuity the loss of lift which gives rise to the trailing vortex occurs only in the neighbourhood of the hinge, as can be seen from the typical chordwise loadings, obtained in electric tank tests, shown in Fig. 4. Therefore the vortex from the discontinuity can be regarded as starting at the hinge, which will normally be between $x = 0{\cdot}5$ and $x = 1{\cdot}0$, and therefore ω_1 appropriate to this vortex $\leqslant 1$. This vortex gives rise to a downwash inboard and an upwash outboard. Inboard the two values of ω_1 appropriate to the tip and discontinuity vortices tend to vary with aspect ratio in opposite directions and the net result is likely to be that there is little or no aspect-ratio effect over the part of the wing with deflected flap: i.e., $\omega = 1$. Outboard of the flap, the upwash from the discontinuity vortex and the downwash from the tip vortex counteract each other. In practice the upwash is greater than

* This statement is based on the results for a 45 deg sweptback wing with full span flaps in Ref. 8, the centres of pressure at mid-semispan being regarded as typical of two-dimensional or unswept conditions. For 35 per cent and 15 per cent chord flaps, c.p. is at $x = 0{\cdot}44$ and $x = 0{\cdot}52$ respectively.

the downwash and there is some lift over the outboard part even when the main wing is at zero incidence. ω_1 associated with the upwash $\leqslant 1$ and ω_1 associated with the downwash $\leqslant 1$, and so outboard of the flap the net result is that $\omega_1 \leqslant 1$. However, the lift outboard of the flap is much less than that over the inner part of the wing and no great error is involved if ω is assumed to be the same for the whole wing as for the inner part, namely unity. For completeness the effect on one half-wing of the trailing vortices from the other half-wing must be considered. In the present case it is easily seen that the above remarks on the downwash factor inboard of the discontinuity apply to the effect of the two vortices from the other half-wing, so that the latter need no special consideration.

Similar arguments apply when the flap extends from the tip inwards to some point along the span. The vortex from the discontinuity now produces a downwash outboard over the part of the wing with flap and an upwash over the inner part which is at zero incidence. Again $\omega_1 \leqslant 1$ for this vortex since the change in lift occurs near the hinge position. However, the tip vortex, which is much stronger in this case than for an inboard flap, now springs from a point approximately at $x = 0{\cdot}5$ so that ω_1 for the tip vortex is about 1 for all aspect ratios. Thus the net result is that ω may not change much with A. As inboard or outboard flaps increase in size towards the limit of a full-span flap, the tip vortex and the discontinuity vortex respectively become weaker and less important and the characteristics of ω tend to those of the full-span flap. For both inboard and outboard flaps ω will increase as the flap chord increases, i.e., as x_v decreases, and this may determine the precise behaviour of ω, i.e., increase or decrease with A. It can be said, however, that the effect of aspect ratio should be small.

There are a number of other possible configurations. For instance the flap need not extend either to centre or tip but could be situated wholly within the half-wing. In this case there would be two discontinuity vortices on each half-wing. Again, the cases dealt with above have assumed symmetrical deflection of the flaps on the two half-wings. It is also possible to have antisymmetrical deflection, as with ailerons, or deflection on one wing only. Such variations can all be dealt with in the same way as the symmetrical deflections. One would guess however that, at least with outboard flaps, the downwash factors would be very similar for symmetrical, antisymmetrical and single deflections. Nowadays inboard ailerons are considered for certain aircraft and thus the case of inboard flaps with antisymmetrical deflection is of interest.

To sum up, on an unswept wing with lift produced by trailing-edge flaps the downwash factor ω will vary less with A than on a wing with lift due to incidence: ω may even be independent of A. Thus in analysing the electrolytic tank results on the basis of Ref. 6 it is important to deduce the appropriate value of ω as well as $\Delta\alpha$.

2.4. *Swept Wings with Deflected flaps.*

Consider first a sweptback wing at zero incidence with full-span trailing-edge flaps. The centre of pressure is about $x = 0{\cdot}5$ over most of the wing, and slightly further forward at the tips. Thus x_v at the tip is greater than on the corresponding wing without flaps, ω_1 is smaller, and ω_2 is roughly the same since it does not vary much with x_v. The total downwash factor $\omega = \omega_1 \times \omega_2$ is therefore less than on the corresponding plane wing, for which the Küchemann formula gave $\omega = 1{\cdot}022$. Compared with the unswept wing with full-span flap, ω_1 is only slightly greater than 1 (since x_v is nearly at $x = 0{\cdot}5$) and ω_2 is appreciably less than 1, so that ω is likely to be less than 1 for a sweptback wing with full-span flap. Moreover ω_1 and ω_2 both tend to increase as A decreases and there should be a noticeable aspect-ratio effect on ω.

Now consider the case of a sweptback wing with part-span flaps extending outwards from the centre section. ω_1 associated with the tip and discontinuity vortices behaves as for the unswept wing in Section 2.3, being greater inboard where there is a flap than it is outboard. In the present case x_v at the tip is slightly less than for an unswept wing so that ω_1 will be slightly greater than 1 inboard of the discontinuity and nearer to 1 outboard. ω_2 inboard does not depend very strongly on x_v and so over the flap the values of ω_2 due to the tip and discontinuity vortices will be similar and the resultant value may not differ much from ω_2 for a wing with full-span flap. Outboard, the value of ω_2 associated with the discontinuity vortex is greater than 1 and the induced velocity here is an upwash. It will be shown in Section 3 that it is possible to take into account in a less direct manner the sweep effect on the downwash from the tip and discontinuity vortices.

In the case of outboard flaps, ω_1 may be slightly less than for inboard flaps since x_v at the tip moves back with the c.p. Over the part of the wing covered by the flap, on which most of the lift is concentrated, ω_2 associated with the strong tip vortex is less than 1 and ω_2 associated with the discontinuity vortex is greater than 1, so that a resultant value over this part of the wing may be in the neighbourhood of 1. As in the case of inboard flaps the effect of sweep on the downwash factor can be incorporated less directly (*see* Section 3).

Like the unswept wing there are other configurations which may be treated by the same approach, but which are not considered here. In particular the results for sweptback wings cannot be applied to swept-forward wings.

To sum up, for a sweptback wing with full-span trailing-edge flap there is likely to be an appreciable variation of ω with aspect ratio and this may also be true for the part-span flaps, but the variation is difficult to estimate without reference to tank data. However, the limit $\omega \to 1$ as $A \to 0$ should be true as for unswept wings with half-chord flaps. The different values of ω on the parts of the wing with and without flaps and for inboard and outboard flaps raise doubts about the validity of the principle of superposition. This will be assumed true later on in the analysis of the electrolytic tank tests but an explicit check of the assumption is very desirable.

2.5. *Application of the Results of Section* 2.

It is emphasised that the results derived in Section 2 are merely qualitative estimates of the factors which affect the downwash on finite wings with flaps, based on very simplified models. Some of these results are used in this note to help in analysing the data from electric tank tests. Confirmation of all the qualitative features and the determination of quantitative relations must depend on such tests. The amount of data at present available is quite small.

3. *The Spanwise Loading of Wings with flaps.*

In calculating by linearized theory the spanwise loadings of wings with flaps it is customary to assume that at any spanwise position the deflection of the flap has added a certain 'equivalent incidence' to the geometric incidence at that section. If this equivalent incidence is known at all spanwise positions the calculation of the spanwise loading can proceed as for a wing without flaps having that particular incidence distribution. The calculations in this Report are based on the methods derived by Multhopp for unswept wings[4]. These equations can be applied to swept wings, as shown by Küchemann[6]. Since in linearized theory the loadings due to incidence, camber, flaps, etc., are additive, it is simplest to calculate a spanwise loading due to flaps only, the main part of the wing being at zero incidence.

In the case of a wing with full-span flap, either swept or unswept, the calculation is of the same type as for a wing without flaps, since the distribution of equivalent incidence over the span is continuous. The appropriate value of ω must be known. In Section 2.3 it was shown that there is likely to be little aspect-ratio effect on the downwash over an unswept wing with full-span flap, so that $\omega = 1$ for all such wings. In Section 2.4, on the other hand, it was shown that ω is likely to be less for a sweptback wing with full-span flaps than for an unswept wing, at least at moderate aspect ratios, but that ω is likely to increase as the aspect ratio of the sweptback wing decreases.

On a wing with part-span flaps the equivalent incidence is discontinuous at one or both ends of the flap and this complicates the spanwise loading calculation. It is still possible, for both swept and unswept wings, to use the method applicable to continuous incidence distributions, but it is almost always necessary to increase the number of spanwise pivotal points Since the work involved increases roughly as the square of the number of points, it is obvious that such a calculation may become too long for a routine method. Moreover, the loading will probably not be accurate in the neighbourhood of the discontinuity, even with the larger number of points.

Multhopp[4] developed a method for dealing with a discontinuity in incidence on unswept wings. (This has been extended by Weber[10] to cover any sort of spanwise discontinuity, e.g. chord.) The incidence distribution is split into two parts, one of which contains the discontinuity, the other being continuous The spanwise loading is then found as the sum of two components γ_I and γ_{II}, both of which are continuous. γ_I is the loading which gives a constant downwash equal to the incidence discontinuity, σ, over

the part of the wing with flap, and zero downwash elsewhere. γ_{II} can be calculated from the remaining incidence distribution. Multhopp gave a theoretical formula for γ_I which was proportional to σ and otherwise depended on the symmetry of the discontinuity and its spanwise position. Some typical γ_I distributions are shown in Fig. 5. Thus in the basic equations

$$\alpha_I = \alpha_{iI} + \alpha_{eI} = \alpha_{iI} + \gamma_I \cdot \frac{2b}{ca} \tag{3}$$

$$\alpha_{II} = \alpha_{iII} + \alpha_{eII} = \alpha_{iII} + \gamma_{II} \cdot \frac{2b}{ca} \tag{4}$$

all the terms in (3) are known except α_I which can therefore be calculated. $\alpha_I + \alpha_{II} = \Delta\alpha$ the equivalent incidence, which is given initially at all spanwise positions. Hence α_{II} is known and continuous and γ_{II} can be calculated as in a normal spanwise loading calculation. Multhopp's work assumes $\omega = 1$ which can be justified for an unswept wing by the reasoning of Section 2.3, even when the aspect ratio is not large. Thus, provided the equivalent incidence is known, Multhopp's method yields adequate results for unswept wings with part-span flaps over a large range of aspect ratios and flap sizes.

Fig. 6 shows a comparison between various calculated spanwise loadings and the electric tank results for an unswept wing of aspect ratio 4, with 20 per cent trailing-edge flaps extending outwards to 0·55 semi-span. In the calculations, the Glauert value of $\Delta\alpha$ at the flap has been corrected slightly by an unpublished theory to allow for the finite aspect ratio. The experimental results were obtained by Professor Malavard in tests[11] previous to the ones analysed in this Report. Fig. 6 shows the difference between the type of calculation using a large number of points and no discontinuity function, and the type of calculation which takes the discontinuity into account. The effect of different values of ω is also shown. The use of the 'plane wing' $\omega = 1{\cdot}054$ makes little difference to the calculation based on $\omega = 1$. The results for 33 per cent flaps show precisely similar characteristics. A comparison in the case of a wing of smaller aspect ratio would be interesting, but no electric tank data is available at present.

Fig. 7 shows results for outboard flaps, asymmetrically deflected, again from Ref. 11. The calculated spanwise loadings are based on $\omega = 1$: this is appropriate for $x_H = 0{\cdot}80$ but a slight increase in ω might be justified for $x_H = 0{\cdot}67$, thus confirming the estimate in Section 2·3 that ω increases as x_H decreases.

The treatment of the discontinuity in the case of sweptback wings is, unfortunately, less straightforward than for unswept wings. To start with, the spanwise distribution of γ_I is such that a strong trailing vortex arises from the discontinuity. Inboard of this vortex, therefore, $\omega_2 < 1$ and outboard $\omega_2 > 1$. This means that Multhopp's expressions for γ_I, derived on the assumption of $\omega = 1$, are not valid for swept wings. Moreover the spanwise variation of ω makes a theoretical derivation of a new γ_I impossible by Multhopp's method and no other theoretical distribution has yet been obtained. Happily the analysis of the electric tank tests has yielded some empirical information on this point, which will be discussed in Section 7. Some idea of the qualitative effect of sweepback on γ_I can easily be gained, however. Over the part covered by an inboard flap the downwash from the discontinuity vortex is less than on the unswept wing, and therefore if the downwash is to be constant and equal to σ the discontinuity must be increased : i.e., γ_I is increased inboard of η_F, the spanwise position of the discontinuity. Outboard of the flap the upwash from the discontinuity vortex will be greater than in the unswept case, and since the net induced vertical velocity in this region must be zero, the downwash from the trailing vortex must also be increased. Therefore over the outer part of the wing γ_I must again be increased, the factor being greater than inboard since it covers the sweep effect and the increase in vortex strength at the discontinuity. In the case of an outboard flap the sweep effect increases the downwash over the flap due to the discontinuity vortex and decreases that due to the tip vortex. As Fig. 3 shows, the net result close to the vortices will be a considerably greater downwash than on the unswept wing and so an overall reduction of γ_I is required. Moreover, the upwash inboard of the flap is reduced by sweep to a greater extent than the downwash from the tip vortex. Thus a relatively stronger discontinuity vortex is required which further reduces γ_I inboard of the flap.

The ω factor for sweptback wings with part-span flaps may therefore be largely incorporated in the

new spanwise loading functions by using the old functions multiplied by a factor, which is >1 for inboard flaps and <1 for outboard flaps. The remainder of the spanwise loading, γ_{II}, is associated with a continuous incidence distribution and the tip vortex is again the strongest. Of course, no chordwise loadings are associated with the components γ_I and γ_{II}, so for the latter it is assumed that the value of ω corresponding to a wing with full-span flap is applicable.

Up to now the equivalent incidence has not been discussed in detail, but this too is more difficult to determine on a swept wing. Nearly 30 years ago Glauert[1] established the linearized theory of thin wings with flaps in two dimensions, which yielded values for the equivalent incidence of a trailing-edge flap of any chord. Subsequent research established exact values for the flat plane with flap[2,3] and various corrections were devised to take account of wing thickness, gap, etc. All this data referred to two-dimensional wings, and the relations so established can be applied fairly confidently to unswept wings provided the aspect ratio is not too small. Theoretical and experimental work[7] on cambered sweptback wings has shown that the zero lift angle of a cambered aerofoil section on a swept wing depends on the angle of sweep and the spanwise position. It thus seems likely that the equivalent incidence of a section with a deflected flap on a swept wing will also depend on the angle of sweep and the spanwise position. Recent theoretical investigations, as yet unpublished, have substantiated this and defined the relationship, but in the present note the experimental data has been analysed to find the equivalent incidence distribution on the wings tested. Some points from the theory crop up occasionally, however.

It has been seen that the downwash factors involved in the spanwise-loading calculations of wings with flaps may differ from the values they have for plane wings of the same planform. However, it is one of the basic assumptions of linearized theory that sectional properties such as the lift slope, a, the chordwise loading parameter, n, and the aerodynamic centre do not depend on the section shape but only on the angle of sweep and the spanwise position. (This implies that incidence, flap and camber terms can be superposed.) Therefore, in the calculations and analysis of this Report, these sectional properties have been calculated as for plane wings.

The data from the electrolytic tank experiments have therefore been analysed to provide information on three points concerning the calculation of the loading on a sweptback wing with flaps:

(i) The value of the downwash factor, ω

(ii) The spanwise variation of the equivalent incidence, $\Delta\alpha$

(iii) The form of the discontinuity function which determines γ_I.

4. *The Arrangements Tested in the Electric Tank*

The electric tank, its uses and technique, have been described by Malavard and Duquenne[9,11]. The present results were obtained by Grandjean and Duquenne[8] at the laboratories of O.N.E.R.A. in Paris and were generously made available to us.

The planform tested was an untapered 45 deg sweptback wing of aspect ratio 4. The wing was represented by a network of 121 electrodes, 11 chordwise at positions

$x = 0{\cdot}025, 0{\cdot}1, 0{\cdot}2, 0{\cdot}3, 0{\cdot}4, 0{\cdot}5, 0{\cdot}6, 0{\cdot}7, 0{\cdot}8, 0{\cdot}9, 1.0$ and 11 spanwise at positions

$\eta = 0, 0{\cdot}1, 0{\cdot}2, 0{\cdot}3, 0{\cdot}4, 0{\cdot}5, 0{\cdot}6, 0{\cdot}7, 0{\cdot}8, 0{\cdot}9, 0{\cdot}975.$

Only inboard flaps, deflected symmetrically about the centreline of the wing, were investigated. Since the apparatus solves Laplace's equation and thus represents the conditions of linearized theory the spanwise loading of wings with outboard flaps deflected symmetrically can be obtained by subtracting the inboard flap results from the full-span flap results provided we accept the principle of superposition. As mentioned earlier (Section 2.4) this ought to be verified for the present configurations. The flaps extended from the centreline to

$$\eta_F = 0{\cdot}25, \quad 0{\cdot}45, \quad 0{\cdot}65, \quad 0{\cdot}85, \quad 1{\cdot}00,$$

the last being a full-span flap. The ratios of flap chord to wing chord were

$$\frac{c_F}{c} = 0{\cdot}15, \quad 0{\cdot}25, \quad 0{\cdot}35:$$

$$\text{i.e. } x_H = 0{\cdot}85, \quad 0{\cdot}75, \quad 0{\cdot}65,$$

where x_H is the x co-ordinate of the hinge. Therefore 15 configurations altogether were investigated. The wings were at zero incidence and the flaps deflected by 1 radian. (In linearized theory the lifting effect of a flap is proportional to the flap deflection.)

The results comprise measurements of the spanwise loadings of the 15 configurations and the chordwise loading of each configuration at the 11 chordwise rows of electrodes from $\eta = 0$ to $\eta = 0{\cdot}975$. So far only the spanwise loadings have been fully analysed to help in the development of a calculation method. The chordwise loadings will be analysed later. Some typical spanwise loadings are shown in Fig. 8, and typical chordwise loadings in Fig. 4.

5. *Methods of Analysing the Results.*

The calculation method of Ref. 6 is used as the basis for the analysis of the electrolytic tank data, since it is necessary to know some of the aerodynamic characteristics of the planform (e.g. the lift slope, a) and also to assist in the extension of the results of the analysis to wings of different sweep, planform and aspect ratio.

The first step is to use the data on full-span flaps to obtain an estimate of the downwash factor ω for these cases, since it is shown in Section 2·4 that it is not easy to make a good enough guess by considering the geometry of the strongest vortices. The spanwise loading data is presented in the form of curves of C_L against η so that $\gamma = C_L.c/2b$ can be found for the spanwise pivotal points of the Multhopp equations, and hence the Multhopp expression for half the downwash at infinity downstream,

$$\alpha_{i0_v} = b_{vv}\gamma_v - \Sigma' b_{vn}\gamma_n$$

can be evaluated. The downwash at the sweptback wing is expressed as

$$\alpha_{i_v} = \omega\alpha_{i0_v}.$$

Using the method of Ref. 6 to calculate the lift slope at the pivotal points, the effective incidence $\alpha_{ev} = C_{L_v}/a_v$ can also be determined at any pivotal point. Therefore if a value can be found for the equivalent incidence, $\Delta\alpha$, ω can be determined from the formula

$$\omega = \frac{\alpha_{i_v}}{\alpha_{i0_v}} = \frac{\Delta\alpha_v - \alpha_{ev}}{\alpha_{i0_v}}$$

In linearized theory the equivalent incidence of a flap on an infinite sheared wing is equal to the Glauert value. In Ref. 11 it is shown that for a two-dimensional wing with flap the tank results agree with the Glauert theory to within 1 or 2 per cent, using 8 chordwise electrodes instead of 11 as in the present tests. Thus it is reasonable to expect that tank results for an infinite sheared wing would also agree with the Glauert theory. At mid-semispan on the wing of aspect ratio 4 conditions are approximately those of a 45 deg sheared wing* so that we can assume $\Delta\alpha$ to be equal to the Glauert value in that region. This leads to the following values for ω:

$x_H = 0{\cdot}65$,	$\omega = 0{\cdot}86$
$0{\cdot}75$,	$0{\cdot}88$
$0{\cdot}85$,	$0{\cdot}80$

There is no consistent variation of ω with x_H and a mean value $\omega = 0{\cdot}85$ has been used for all three flap chords and assumed to be constant over the whole span. This value for ω confirms the qualitative estimate of Section 2.4.

---

* In fact there was a small aspect-ratio effect noticeable: the unpublished theoretical calculations of $\Delta\alpha$ have been used to make the very slight modification necessary to the Glauert values.

The next step is to use this value of ω to calculate the value of $\Delta\alpha$ at all the remaining pivotal points, rearranging the above formula:

$$\Delta\alpha_v = \alpha_{ev} + \omega\alpha_{i0_v}$$

Finally we examine the data for the part-span flaps using the newly-found values of ω and $\Delta\alpha$ to help to determine the appropriate spanwise functions γ_I and their relationship to the corresponding functions for unswept wings. The procedure is as follows:

γ_v is known at the pivotal points and

$\gamma_v = \gamma_{Iv} + \gamma_{IIv}$.

By the Multhopp equations,

$$\gamma_{IIv}\left(b_{vv} + \frac{2b}{\omega a_v c_v}\right) = \frac{\alpha_{IIv}}{\omega} + \Sigma' b_{vn}\gamma_{IIn}$$

$$= \frac{\alpha_v - \alpha_{eIv} - \alpha_{iIv}}{\omega} + \Sigma' b_{vn}\gamma_{IIn}$$

$$= \frac{\alpha_v - \alpha_{iIv}}{\omega} - \frac{2b}{\omega\alpha_v c_v}\gamma_{Iv} + \Sigma' b_{vn}\gamma_{IIn}$$

$$= \frac{\alpha_v - \alpha_{iIv}}{\omega} - \frac{2b}{\omega a_v c_v}\left(\gamma_v - \gamma_{IIv}\right) + \Sigma' b_{vn}\gamma_{IIn}$$

therefore

$$\gamma_{IIv} b_{vv} = \left(\frac{\alpha_v - \alpha_{iIv}}{\omega} - \frac{2b}{\omega a_v c_v}\gamma_v\right) + \Sigma' b_{vn}\gamma_{IIn}.$$

γ_{II} may be found by iteration, since

$$\alpha_v = \Delta\alpha_v \text{ on the flap}$$
$$= 0 \text{ outside the flap}$$

and

$$\alpha_{iIv} = -\sigma \text{ inboard of the discontinuity}$$
$$= 0 \text{ outboard}$$

σ is the discontinuous jump in incidence and is equal to the value of $\Delta\alpha$ at the end of the flap

b, c_v, a_v, are already known

ω is assumed to have the same value as for the wing with full-span flap in accordance with the estimate in Section 2.4. Hence γ_I may be found from

$$\gamma_I = \gamma - \gamma_{II}$$

We may write for a wing swept back by an angle φ.

$$[\gamma_I(\eta)]_\varphi = [\tau(\eta)]_\varphi \times [\gamma_I(\eta)]_0,$$

assuming the same value for σ on both swept and unswept wings. $\tau(\eta)$ depends on sweepback, flap span and flap chord, as well as on η. At present $\tau(\eta)$ cannot be obtained theoretically. Thus for an unswept wing

$$[\gamma(\eta)]_0 = [\gamma_I(\eta)]_0 + [\gamma_{II}(\eta)]_0$$

and for a sweptback wing

$$\begin{aligned}[\gamma(\eta)]_\varphi &= [\gamma_I(\eta)]_\varphi + [\gamma_{II}(\eta)]_\varphi \\ &= \tau(\eta)[\gamma_I(\eta)]_0 + [\gamma_{II}(\eta)]_\varphi .\end{aligned}$$

The relation between α_i and $\gamma(\eta)$ for an unswept wing

$$\alpha_i = \frac{\omega_0}{2\pi}\int_0^1 \frac{d\{[\gamma_I(\eta')]_0 + [\gamma_{II}(\eta')]_0\}}{d\eta'} \cdot \frac{d\eta'}{\eta - \eta'}$$

has become for a swept wing

$$\alpha_i = \frac{1}{2\pi}\int_0^1 \frac{d\{\tau(\eta') \cdot [\gamma_1(\eta')]_0 + [\gamma_{II}(\eta')]_\varphi\}}{d\eta'} \cdot \frac{d\eta'}{\eta - \eta'} .$$

Since the tank tests give results corresponding to linearized theory the spanwise loading of outboard flaps can be obtained as the difference of the spanwise loadings of the complementary inboard flaps and the full-span flaps, with the proviso noted in Section 4. Therefore $\tau(\eta)$ can also be found for swept wings with outboard flaps symmetrically deflected. The case of antisymmetrical deflection cannot be dealt with explicitly from existing data but Section 8 will show that the factors for symmetrical deflection give reasonable results for the other configuration.

6. *Results for the Equivalent Incidence, $\Delta\alpha$*

The values of $\Delta\alpha$ found by analysis of the electrolytic tank data for full-span flaps are plotted against η in Fig. 9, for each of the flap-chord ratios. The results are plotted as $\Delta\alpha/\beta$ since β, the flap deflection, was unity (1 radian). Theoretical considerations indicate that $\Delta\alpha$ decreases near the centre of a sweptback wing and increases near the tip compared with the Glauert value for two-dimensional and sheared wings.

There is a good deal of scatter in the analysed values of $\Delta\alpha$ for all three flap chords. It is not possible to draw a smooth curve through any set of points. In Fig. 9 two curves are drawn through each set. The full lines are obtained by interpolating $\Delta\alpha$ between the sheared wing value and the values at $\eta = 0$ and $\eta = 0{\cdot}981$ in accordance with the 'λ-curve' of Ref. 6 which governs some of the centre and tip variations on swept wings. For $x_H = 0{\cdot}85$ $\Delta\alpha$ increases towards the tip whereas for $x_H = 0{\cdot}65$ and $0{\cdot}75$ it decreases. The dotted lines are the theoretical values of $\Delta\alpha$ from the unpublished theory referred to earlier, and for all three values of x_H, $\Delta\alpha$ increases towards the tip. The following conclusions may be drawn from Fig. 9:

(i) At mid semi-span $\Delta\alpha$ is equal to the Glauert value, the downwash factor having been chosen to make this so.

(ii) $\Delta\alpha$ decreases towards the centre of the wing.

(iii) At the centre the analysed values of $\Delta\alpha$ are greater than the theoretical values.

(iv) If anything, the analysed values from $\eta = 0{\cdot}195$ to $\eta = 0{\cdot}707$ are closer to the theoretical curve than to the λ-interpolation curve.

(v) The analysed values of $\Delta\alpha$ near the tip tend to decrease rather than increase.

In previous electrolytic tank results for sweptback cambered wings[12] it has been noted that there is a discrepancy between the centre and tip effects on the spanwise loading as measured in the tank and that calculated by the method of Ref. 7. The same sort of discrepancy is apparent here, the theoretical $\Delta\alpha$ being less at the centre section and greater near the tip. The discrepancies have not yet been explained. $\Delta\alpha$ is obtained from the tank data by determining α_i and α_e. α_{i0} is small at the centre section and quite large changes in ω have little effect on the sum $\alpha_i + \alpha_e$: therefore the choice of downwash factor is not responsible at the centre. Near the tip the gap between tank results and theoretical calculations is even more pronounced since $\Delta\alpha$ at $\eta = 0{\cdot}832$ and $\eta = 0{\cdot}924$ varies in the opposite direction to that expected. The three points for $\eta = 0{\cdot}981$ are not systematic but the odd point is the one which is greater than the Glauert value and which therefore behaves as theory would predict. In this case it is possible to argue that ω should increase locally near the tip, since ω_2 increases close to its associated vortex (*see* Fig. 3). If ω is allowed to increase in a suitable manner to 1·00 at the tip, $\Delta\alpha$ at $\eta = 0{\cdot}981$ is increased to a value more in agreement with theory. These points are shown flagged in Fig. 9. At $\eta = 0{\cdot}832$ and $\eta = 0{\cdot}924$, however, $\Delta\alpha$ is still well below the expected value.

It is now clear that the analysed values of $\Delta\alpha$ are extremely sensitive to the accuracy of the data and to the assumptions of the theory used in the analysis, especially near the tips. It seems unlikely that more accurate values of $\Delta\alpha$ can be deduced from experiments without introducing most unwelcome complications in the simple basic theory. Fortunately it is conversely true that the spanwise loading is not very sensitive to the variation of $\Delta\alpha$ with η, so that for practical purposes extreme accuracy in the equivalent incidence is not necessary. Fig. 10 shows a comparison between the measured spanwise loading of one of the wings and that calculated using the theoretical $\Delta\alpha$ values. In view of the big discrepancies in $\Delta\alpha$ at the centre and tips the differences in the spanwise loading are comparatively modest. Nevertheless more research to try to reconcile theory with experiment is desirable.

7. *Results for the Spanwise Loading functions with Discontinuity.*

The method of Section 5 to determine the spanwise loading function has been applied to all the present tank data on 45 deg sweptback wings with part-span flaps. The values of $\Delta\alpha$ were obtained from the full-span flap data as follows:

For each flap chord $\Delta\alpha$ was assumed to have the Glauert value at mid semi-span, and the analysed value at the centre, intermediate points lying on the λ- interpolation curve, the full lines of Fig. 9. For $x_H = 0{\cdot}65$, near the tip, $\Delta\alpha$ is assumed to have the analysed value at $\eta = 0{\cdot}981$ and intermediate points given by the λ-interpolation curve. For $x_H = 0{\cdot}75$ and 0·85 the $\Delta\alpha$ variation near the tip has been systematized to give the same proportional increase in $\Delta\alpha$ as for $x_H = 0{\cdot}65$. These curves are shown in Fig. 9. Hence, for example, at $\eta_F = 0{\cdot}85$, $\Delta\alpha/\beta = 0{\cdot}736$ for $x_H = 0{\cdot}65$, 0·646 for $x_H = 0{\cdot}75$ and 0·527 for $x_H = 0{\cdot}85$.

The resulting values of $\tau(\eta)$, the sweep factor to the spanwise loading function γ_I (assuming the same value of σ with and without sweep), are shown in Table I and in Figs. 12 to 14. As expected from Section 3, $\tau(\eta)$ for the inboard flaps is greater than unity and is greater outboard of the flap than over the flap itself. The limit as $\eta_F \to 1{\cdot}00$ is $\tau(\eta) = 1/\omega$, shown dotted for $\omega = 0{\cdot}85$. For a given flap chord, $\tau(\eta)$ increases as η_F decreases, and for a given η_F, $\tau(\eta)$ increases as the flap chord decreases. This agrees with the conclusion of Section 2.3 about inboard flaps on unswept wings, since $\tau(\eta)$ is inversely proportional to ω. For the outboard flaps $\tau(\eta)$ is less than unity and is less inboard of the flap than over the flap itself. As in the case of inboard flaps, $\tau(\eta)$ increases as η_F decreases for a given flap chord. For a given η_F, $\tau(\eta)$ decreases as the flap chord decreases. This is contrary to the conclusion of Section 2·3 for outboard flaps on unswept wings. In the present case the behaviour is chiefly determined by ω_2 outboard of the discontinuity, which increases as the flap chord decreases: whereas ω_1 decreases as the flap chord decreases.

In view of all the possible sources of inaccuracy the curves of $\tau(\eta)$ against η are well-defined and systematic, and are presented as being suitable for use in spanwise loading calculations of 45 deg sweptback wings. An extension to other values of sweepback angle is suggested in the next Section.

8. *Application of the Results to Other Configurations.*

The results obtained by analysis of the electrolytic tank tests refer to constant-chord wings of 45 deg sweepback, aspect ratio 4, with flaps of various sizes. The results of the analysis comprise:

(i) A value of ω for the wings with full-span flaps (also applicable to some calculations) with part-span flaps).

(ii) A set of values of $\Delta\alpha$ on the wings with full-span flaps.

(iii) A set of values of the spanwise loading factor $\tau(\eta)$, which depends on x_H and η_F.

We wish to extend these results to cover other wing configurations, e.g. different flap sizes, different sweep angles. The only other electrolytic tank data on swept wings with flaps is for constant-chord wings of 30 deg and 45 deg sweepback, $A = 4^{11}$. We will use these results to support some suggested interpolation formulae between $\varphi = 0$ deg and 45 deg for ω, $\tau(\eta)$, etc.

Consider first the extension of the present results for wings of 45 deg sweep to other wings of the same planform but with different flap sizes. ω may be left unchanged, at least for $0{\cdot}65 \leqslant x_H \leqslant 0{\cdot}85$. Within this range of flap chords $\Delta\alpha$ may be simply interpolated graphically, as also may $\tau(\eta)$ for $0{\cdot}65 \leqslant x_H \leqslant 0{\cdot}85$ and $0{\cdot}25 \leqslant \eta_F \leqslant 1{\cdot}00$.

Turning now to wings of different sweepback, we try to find the appropriate value of ω. ω is mainly dependent on $\omega_2 = 1 - \sin\varphi$ in the limit. We may therefore guess

$$[\omega]_{\varphi \text{ II } 0^0} - [\omega]_\varphi \propto \sin\varphi$$
$$= K \sin\varphi$$

as an interpolation formula. We know that $[\omega]_{\varphi=0^0} = 1$ (*see* Section 3) and

$$1 - [\omega]_{45^0} = 0{\cdot}15 = 0{\cdot}707 \times K,$$

so that $K = 0{\cdot}212$. This gives

$$[\omega]_\varphi = 1 - 0{\cdot}212 \sin\varphi \tag{5}$$

Another possible interpolation is

$$1 - [\omega]_\varphi \propto \varphi = K . \varphi$$

We know that $0{\cdot}15 = K . \frac{\pi}{4}$ so that $K = 0{\cdot}191$ and

$$[\omega]_\varphi = 1 - 0{\cdot}191 . \varphi \tag{6}$$

φ being measured in radians. Yet another possible interpolation is to assume

$$1 - [\omega]_\varphi \propto \{[\omega_K]_{\varphi=0^0} - [\omega_K]_\varphi\}$$

where ω_K is the Küchemann factor for a plane wing given by equations (1) and (2). We know that $0{\cdot}15 = K \times 0{\cdot}032$ so that $K = 0{\cdot}47$ and

$$[\omega]_\varphi = 1 - 0{\cdot}47\{[\omega_K]_{\varphi=0^0} - [\omega_K]_\varphi\} \tag{7}$$

For a wing of 30 deg sweepback and aspect ratio 4 we get the following results:

$$\omega = 0{\cdot}89 \text{ by equation (5)}$$
$$= 0{\cdot}90 \text{ by equation (6)}$$
$$= 0{\cdot}91 \text{ by equation (7)}$$

Unfortunately no data is available for full span flaps other than those for the 45 deg wing and so no direct confirmation of any of these formulae is possible. We will take $\omega = 0{\cdot}90$ as being applicable to 30 deg sweep.

For smaller sweep angles, the three equations (5) to (7) are in even closer agreement: for $\phi = 15$ deg each gives $\omega = 0{\cdot}95$.

To derive $\Delta\alpha$ for a wing of different sweep we use the parameter n (Ref. 6) which is a function both of sweep and spanwise position as is $\Delta\alpha$. For a wing with sweepback angle equal to ϕ, the general equation for n is

$$n = 1 - \frac{1 + \dfrac{\lambda\varphi}{\pi/2}}{2\left\{1 + \left(\dfrac{a_0 \cos\varphi}{\pi A}\right)^2\right\}^{\frac{1}{4\left(1+\frac{|\varphi|}{\pi/2}\right)}}}$$

where the symbols have the same meaning as elsewhere in this report. The Küchemann value of the downwash factor ω for wings without flaps is equal to twice the value of n at the sheared part of the wing where $\lambda = 0$, as is clear from equation (2) in Section 2.2. Theoretical considerations indicate that the complete dependence of $\Delta\alpha$ on sweep and spanwise position can be expressed in terms of n. The $\Delta\alpha/\beta$ curves of Fig. 9 have therefore been replotted against n in Fig. 11. On the 45 deg swept wings n (allowing for small aspect-ratio effects) is equal to 0·273 at the centre and 0·748 at the tip. Thus the range of n covered is applicable to wings of similar aspect ratio having angles of sweep between 0 deg and 45 deg, and $\Delta\alpha$ may be determined for any spanwise position on such wings. The curves for $x_H = 0{\cdot}75$ and $x_H = 0{\cdot}85$ appear to be unreliable beyond $n = 0{\cdot}6$ and the dotted curves may be more useful in that region. (These have been used in estimating $\tau(\eta)$, as mentioned in Section 7).

To make an estimate of $\tau(\eta)$ for a wing of any sweep, we remember that $\tau(\eta)$ differs from unity because of the sweep effect on the downwash factor. We assume that the difference between $\tau(\eta)$ and unity for $\eta_F < 1$ is proportional to that difference for $\eta_F = 1$, i.e. a full-span flap, and $\tau(\eta)$ for a full-span flap $= 1/\omega$. Thus for two comparable wings of sweep φ_1 and φ_2, with inboard flaps:

$$\frac{[\tau(\eta)]_{\varphi_1} - 1}{[\tau(\eta)]_{\varphi_2} - 1} = \frac{\dfrac{1}{[\omega]_{\varphi_1}} - 1}{\dfrac{1}{[\omega]_{\varphi_2}} - 1}$$

i.e.
$$[\tau(\eta)]_{\varphi_1} = 1 + \frac{\dfrac{1}{[\omega]_{\varphi_1}} - 1}{\dfrac{1}{[\omega]_{\varphi_2}} - 1} \cdot \{[\tau(\eta)]_{\varphi_2} - 1\}. \qquad (8)$$

If $\varphi_1 = 30$ deg, $\varphi_2 = 45$ deg,

$$[\tau(\eta)]_{30^\circ} = 1 + \frac{\frac{1}{0{\cdot}90} - 1}{\frac{1}{0{\cdot}85} - 1} \cdot \{[\tau(\eta)]_{45^\circ} - 1\}$$

$$= 1 + 0{\cdot}61\{[\tau(\eta)]_{45^\circ} - 1\} \ . \tag{9}$$

To check equations (5) to (8) and Fig. 11 the spanwise loading has been calculated for the wings of Ref. 11 having $\varphi = 30$ deg, inboard flaps, $\eta_F = 0{\cdot}55$, $x_H = 0{\cdot}67$ and $0{\cdot}80$. The results of Ref. 11 were obtained by an earlier electrolytic tank procedure using 8 chordwise electrodes instead of 11 as in the present tests. As a datum, therefore, the spanwise loading was first calculated for the wings of 45 deg sweep with the above flap sizes using $\Delta\alpha$ and $\tau(\eta)$ from the present tests. The comparison with the tank data is shown in Fig. 15 and the calculation is seen to give a slightly higher loading than the tests. The comparison for the 30 deg wings is given in Fig. 16 which shows that the calculated and experimental loadings differ exactly as for $\varphi = 45$ deg. It is concluded that the discrepancy in the results of Fig. 15 for $\varphi = 45$ deg is due to the differences between the 8-point and 11-point tank data and that the interpolation formulae (5) to (8) give a satisfactory correspondence for $\varphi = 30$ deg in Fig. 16. The differences between the two sets of tank data for $\varphi = 45$ deg underline the remark made in the Introduction that a fairly large number of chordwise points are required to represent the wing by a 'lattice'.

For a wing with outboard flaps, symmetrically deflected, the interpolation formula corresponding to equation (8) is

$$[\tau(\eta)]\varphi_1 = 1 - \frac{\frac{1}{[\omega]_{\varphi_1}} - 1}{\frac{1}{[\omega]_{\varphi_2}} - 1} \cdot \{1 - [\tau(\eta)]_{\varphi_2}\} \tag{10}$$

since $\tau(\eta)$ is now less than unity, in general. If $\varphi_1 = 30$ deg, $\varphi_2 = 45$ deg,

$$[\tau(\eta)]_{30^\circ} = 1 - 0{\cdot}61\{1 - [\tau(\eta)]_{45^\circ}\} \tag{11}$$

Apart from those used in the present analysis, no tank data are available on wings with outboard flaps symmetrically deflected, but Ref. 11 contains data on outboard flaps with anti-symmetrical deflection for $\varphi = 0$ deg, 30 deg and 45 deg. (The results for $\varphi = 0$ deg have already been shown in Fig. 7.) The spanwise loading of the wings of 30 deg and 45 deg sweepback has been calculated, using the $\tau(\eta)$ curves for $\varphi = 45$ deg, outboard flaps symmetrically deflected, and equation (10). The results for $\varphi = 45$ deg are given in Fig. 17 and for $\varphi = 30$ deg in Fig. 18. From Fig. 17 it is clear that the $\tau(\eta)$ factors for symmetrical deflection are not strictly applicable to cases of anti-symmetrical deflection, and Fig. 18 shows that the interpolation equation (10) may not be valid either. Figs. 17 and 18, like Fig. 7, show that a larger variation of ω with x_H might be appropriate. This would imply that, for a given η_F, the $\tau(\eta)$ curves for anti-symmetrical deflection would vary more with x_H than for symmetrical deflection. Nevertheless the calculation is in fair agreement with experiment and the method is certainly worth using until electrolytic tank tests furnish more explicit information.

Anti-symmetrical deflection of inboard flaps has not been treated. The system of vortices will be different from any considered so far. Only a qualitative discussion on the lines of Section 2 is possible at present.

In general, small aspect-ratio effects are just beginning to appear with these wings of $A = 4$. The results of the present analysis should be applicable to wings of greater aspect ratio. The $\Delta\alpha$ curves, plotted against n, should also be valid for wings of smaller aspect ratio. The $\tau(\eta)$ factors will change as the aspect ratio is reduced, however, and further data are required before this variation can be found and an interpolation formula developed. The qualitative discussion of Sections 2.3 and 2.4 suggest that there should be little aspect-ratio effect on unswept wings but an appreciable effect on swept wings. Thus the extension of the results of the present analysis to wings of different aspect ratio can, for the time being, only be justified for $A > 4$.

No suitable tank tests are available for checking the effect of taper on the spanwise loading of swept wings with flaps. It is suggested that the angle of sweep of the mid-chord line be used in calculations. It should be noted that the flap chord ratio may change along the span and that quantities expressed in terms of the chord are now in terms of the local chord. Where the flap chord ratio varies, a composite $\tau(\eta)$ curve is required. It is suggested that at the spanwise pivotal points $\tau(\eta)$ should be based on the local flap chord, and that outside the flap $\tau(\eta)$ should be based on the flap chord at the discontinuity.

9. *Calculation procedure.*

As a result of the analysis of the electrolytic tank tests it is possible to suggest a method for calculating the spanwise loading on a swept wing with deflected hinged trailing edge flaps, and this section summarizes the procedure. The method, which is based on the linearized theory of incompressible flow, is regarded as an extension of earlier methods[6, 7] developed for plane and cambered wings, and the fundamental ideas and assumptions are unchanged. The loading in compressible flow below the critical Mach number may be obtained by using the Prandtl-Glauert analogy in which the spanwise dimensions are reduced by the factor $\sqrt{1-M_0^2}$ and the loading of the modified configuration calculated in incompressible flow[6].

As in the case of a plane wing, the first step in the calculation of the spanwise loading is to determine the local lift slope, a, at the spanwise pivotal points from the formula of Ref. 6. Since we treat the incidence discontinuity by Multhopp's method, 15 pivotal points on the whole wing are sufficient, i.e. 8 on a half-wing. The spanwise variation of the parameter n is found in the course of the calculation of a and so $\Delta\alpha$ at the pivotal points and the discontinuities can be found from Fig. 11 for x_H between 0·65 and 0·85. It is suggested that the dotted lines near the tip in Fig. 11 are more likely to be reliable than the full curves. The curves could be extrapolated to cover nearly all required values of n.

The spanwise distribution of $\gamma = C_L c/2b$ is calculated as the sum of two component distributions, γ_I and γ_{II} (*see* Section 5). γ_I depends on the angle of sweep and on the magnitude and spanwise position of the incidence discontinuity at the end of the flap. Multhopp's formulae for γ_I for inboard and outboard flaps on an unswept wing are given in Appendix II. On a wing swept back by an angle φ, the spanwise loading function $[\gamma_I(\eta)]_\varphi$ is given by

$$[\gamma_I(\eta)]_\varphi = [\tau(\eta)]_\varphi \times [\gamma_I(\eta)]_{0^\circ}$$

so that $\alpha_{iI} = \sigma$ (the incidence discontinuity) over the flap and zero elsewhere and for $\varphi = 45$ deg, $\tau(\eta)$ is presented in Table I and Figs. 12 to 14, for various flap spans and chords, with symmetrical deflection. $[\tau(\eta)]_{45^\circ}$ for other flap sizes may be obtained by interpolation, and for a change in sweep angle $[\tau(\eta)]_\varphi$ is obtained from $[\tau(\eta)]_{45^\circ}$ by equations (8) or (10) in Section 8: for inboard flaps, equation (8) is used:

$$[\tau(\eta)]_\varphi = 1 + \frac{\dfrac{1}{[\omega]_\varphi} - 1}{\dfrac{1}{[\omega]_{45^\circ}} - 1} \{[\tau(\eta)]_{45^\circ} - 1\}$$

and for outboard flaps equation (10) is used:

$$[\tau(\eta)]_\varphi = 1 - \frac{\frac{1}{[\omega]_\varphi} - 1}{\frac{1}{[\omega]_{45°}} - 1} \{1 - [\tau(\eta)]_{45°}\}.$$

Until further data is available it is suggested that $\tau(\eta)$ for outboard flaps symmetrically deflected may also be used in the case of anti-symmetrical deflection without serious error. Thus the function γ_I may be calculated for a wide range of configurations.

It is preferable to calculate the spanwise loading due to flaps with the main part of the wing at zero incidence. The result can then be added to the spanwise loading due to incidence to give any desired combination of flap deflection and incidence angle. At the flap the local incidence is $\Delta\alpha$, elsewhere it is zero, the incidence discontinuity σ being the value of $\Delta\alpha$ at the end of the flap. Thus the geometric incidence α is known everywhere. To calculate γ_{II} we must know the associated incidence distribution $\alpha_{II} = \alpha - \alpha_I$. The effective incidence α_{eI} associated with γ_I is $\frac{C_{LI}}{a} = \frac{2b}{ac} \cdot \gamma_I$ which is known: also the induced incidence

α_{iI} associated with γ_I has been specified to be equal to σ over the flap and zero elsewhere. Hence $\alpha_{II} = \alpha - (\alpha_{eI} + \alpha_{iI})$ and γ_{II} can be calculated by the usual Multhopp-type equations

$$\gamma_{II_\nu} \left(b_{\nu\nu} + \frac{2b}{\omega a_\nu c_\nu} \right) = \frac{\alpha_{II_\nu}}{\omega} + \Sigma' b_{\nu n} \gamma_{II_n}$$

which can be solved by iteration. In these equations and in the interpolation formulae for $\tau(\eta)$, ω is obtained from equations (5), (6) or (7) of Section 8:

$$[\omega]_\varphi = 1 - 0{\cdot}21 \sin \varphi$$

or

$$[\omega]_\varphi = 1 - 0{\cdot}19\, \varphi$$

or

$$[\omega]_\varphi = 1 - 0{\cdot}47\{[\omega_K]_{0°} - [\omega_K]_\varphi\}$$

for the present range of x_H. The sum of γ_I and γ_{II} gives the spanwise loading, γ.

The above calculation method does not depend on the values of ω, $\tau(\eta)$ and $\Delta\alpha$ given in this note, and if more accurate values are subsequently available they can be inserted. The $\tau(\eta)$ curves of Figs. 12 to 14 are unlikely to be valid for aspect ratios less than 4 and ω may also change A is decreased.

In the case of a tapered wing the angle of sweep of the mid-chord line should be used. Since x_H may vary with spanwise position, $\tau(\eta)$ may have to be considered for each pivotal point separately (*see* Section 8).

10. *All-Moving Tip Controls*

A problem closely allied to that of the loading of swept wings with flaps is to find the loading of wings with all-moving tip controls. Such controls appear to give promising results especially in the transonic range and their effect has recently been discussed by Thomas and Mangler[13]. This paper also contains a method for calculating the spanwise loading at subsonic speeds. No electric tank data on all-moving tips exist at present and so no direct check of the method of Ref. 13 can be made. It is of interest however, to compare the results of Ref. 13 with a calculation on the lines of the present Report, since the remarks in the Introduction about Multhopp's more recent paper[5] apply to the method of Thomas and Mangler, namely:

(i) The number of chordwise points is too limited and the method of their selection too uncertain to give reliable results.

(ii) The spanwise discontinuity in incidence cannot be split off and 15 spanwise points with a continuous incidence distribution does not give a good representation (*see* Fig. 6). In Ref. 13 two methods are quoted for fairing over the discontinuity region and the difference between the two is quite appreciable.

In Ref. 13 the calculations are made for delta planforms and an example of this type with pointed tips, $A = 1{\cdot}848$, leading-edge sweep of 65·2 deg, $\eta = 0{\cdot}67$ and $0{\cdot}74$ is used for a comparison of the methods.

The three things which must be known to perform a calculation by the present method are $\Delta\alpha$, ω and $\tau(\eta)$. In this example $\Delta\alpha$ is known since it is equal to the control deflection β and $\Delta\alpha/\beta = 1$. (This can be regarded as the case $x_H = 0$). No experimental data are available from which ω and $\tau(\eta)$ can be obtained for this value of x_H and a plausible guess must be made. As both parts of the wing can be considered as a wing at incidence we assume that ω is given by equation (2) as for a plane wing at incidence, which means that $\omega = 1{\cdot}080$. Thus $\tau(\eta) = \dfrac{1}{\omega} = 0{\cdot}925$ is probably an upper limit to the spanwise loading factor, and by analogy with Figs. 12 to 14 it will probably be reasonably correct for the outer part of the wing which carries most of the load. On these assumptions the spanwise loading has been calculated for unit control deflection, the main part of the wing being at zero incidence. The results are shown as curve (*a*) of Figs. 19 and 20.

In view of the shape of the spanwise loading curve it can be argued that the tip control should be considered as a wing of half the aspect ratio of the complete wing. Curve (b) in Fig. 19 shows the effect of calculating ω on the basis of $A = 0{\cdot}924$ with $\tau = 1/\omega$. There is an overall increase in loading, probably rather spurious inboard of the control since the new assumption about A is hardly valid there. Therefore, although the maximum uncertainty about the value of A has been considered, the results do not differ much in the two cases.

Finally, for comparison purposes, the loading on the control has been calculated assuming a full reflection at the inboard end and this is shown dotted in Figs. 19 and 20. There is, of course, no load inboard of the control in this extreme treatment.

Curves (c) and (d) in Figs. 19 and 20 have been reproduced from Ref. 13, and show the effect of the uncertainty about how to fair the incidence in between the spanwise pivotal points. Two methods have been suggested in Ref. 13 and the difference between the results (c) and (d) is greater than between curves (a) and (b), and for the two control sizes the difference is not consistent in sign.

There is a considerable difference between the two sets of results which cannot be explained physically. To get closer agreement with (c) and (d) the calculations by the present method would have to use a smaller value of ω (i.e. an aspect ratio greater than that of the complete wing): or would have to assume that $\tau > 1/\omega$ which cannot be justified by the analysis of the electrolytic tank results. Thus the two methods cannot at present be reconciled.

The discrepancy is more serious in the pitching and rolling moments. This makes an estimate of the control efficiency of all-moving tips at subsonic speeds uncertain. Fig. 21 gives the various results for the spanwise variation of the aerodynamic centre. Not all the difference is due to the tip deflection: there is a large discrepancy in the values for the plane wing at incidence. Similar differences have been noted before in Ref. 6 where it has been suggested that Multhopp's more recent method[5] is liable to overestimate the centre effect on sweptback wings. Among other things this tends to place the aerodynamic centre too far back.

From the calculated spanwise loadings the overall values for the lift and the rolling moment have been evaluated. They are given in Table 2. The difference between the various sets of results are quite large.

The above results by both methods are for inviscid, incompressible flow with the trailing vortices lying in a plane sheet. There are several effects which might modify these results. For instance the gap between the main wing and the tip might give rise to a vertical sheet of trailing vortices. This would change the downwash due to the trailing vortices and might cause a partial reflection effect near the discontinuity similar to that found with wing fences[14]. The partial reflection might not only affect the lift distribution but also cause a rearward shift of the aero-dynamic centre on the control, as indicated

by the curve for full reflection in Fig. 21. Again, the gap is almost certain to interfere with the development of the part-span vortex sheet in the same way as a chord extension or a notch, and ordinary boundary-layer effects will also influence the loading to a large extent.

If these viscosity effects are to be found they must come from experimental results and they cannot be estimated with any certainty unless the inviscid solution is known. It is therefore of importance that reliable calculation methods be devised for flaps and all-moving tip controls.

11. *Conclusions and Further Work.*

At the outset of the present investigation it was hoped that a limited number of configurations tested in an electrolytic tank would yield results which could be generalised to cover any system of trailing-edge flaps on wings of any sweepback. The main object was to see whether $\Delta\alpha$ varied in a spanwise direction on a swept wing, and if so to obtain curves of $\Delta\alpha$ between centre and tip and relate these to the flap chord and the parameter n of Ref. 6. In the course of the analysis it became clear that there were other effects of sweep which could be inferred by qualitative reasoning but whose magnitude could not be predicted. In particular, both the downwash factor ω and the Multhopp spanwise loading function γ_I for wings with a discontinuity of incidence exhibited variations with sweep which had to be estimated by a study of the electrolytic tank results. The relation between α_{iII} and γ_{II} remained as before.

The main conclusions to be drawn from the analysis are:

(i) The downwash factor, ω, on swept wings may differ from unity even on wings of high aspect ratio: and on both swept and unswept wings the variation of ω with aspect ratio may depend on the chordwise loading.

(ii) Using the theory of Ref. 6 as a framework it is possible to deduce values of $\Delta\alpha$ over the span of a swept wing with full-span flaps, but these values are very sensitive to the accuracy of the tank data and the initial assumptions such as the value of ω. Since the ω relations are even more complicated in the case of part-span flaps, tests on these configurations are not useful for determining $\Delta\alpha$.

(iii) If $\Delta\alpha$ is known from full-span flap data, then for swept wings with part-span flaps the ω values can be obtained from the test results in the form of a spanwise loading factor, $\tau(\eta)$, to the Multhopp spanwise loading function γ_I.

(iv) A method for calculating the spanwise loading due to flap deflection is presented in which the above results can be inserted. Subsequent corrections or modifications to $\Delta\alpha$, ω and $\tau(\eta)$ can be applied without difficulty. In particular when corrections to $\Delta\alpha$ are available to allow for profile thickness, boundary layer, etc., they may be easily incorporated.

The spanwise loading of a delta wing with all-moving tip control has been calculated by this method and the results do not agree with those of Ref. 13. The discrepancies have yet to be explained.

An analysis of the chordwise loading results of the present series of tank tests has started and this should lead to a calculation method for the chordwise loading on swept wings with flaps, and will serve as a check on some theoretical ideas.

A theoretical derivation of the variation of $\Delta\alpha$ with sweep has been tackled, and it is just possible that $\tau(\eta)$ may also be derived from theory. Practical values of ω however must always be obtained from analogue computer data, owing to the very complex vorticity distributions on the wings. It is therefore suggested that further work to provide such data is needed along the following lines:

(i) Theoretical derivation of spanwise loading factor $\tau(\eta)$, if possible.

(ii) Electrolytic tank tests on unswept wings of various small aspect ratios with full-span and part-span (inboard and outboard) flaps, to check any variation of ω_1 with A for these chordwise loadings.

(iii) Tank tests on wings of the same sweep but different aspect ratios, with full-span and part-span flaps, to check the variation of ω with A.

(iv) Tank tests on wings of the same aspect ratio but different sweep angles, to check the interpolation formulae for $\tau(\eta)$ and ω given in the present Report.

(v) Tank tests on wings with outboard flaps to check the additive property of spanwise loadings in linearized theory.

(vi) Tank tests on inboard and outboard flaps with antisymmetric loadings to ascertain the appropriate spanwise variation of $\tau(\eta)$.

(vii) Tank tests on tapered wings and delta wings with various flap configurations to ascertain the appropriate sweep angle to use in such calculations.

(viii) Tank tests on wings with all-moving tips, particularly swept wings.

(ix) Tank tests on wings with nose flaps.

Of these items, Nos. (ii), (iii), (v) and (viii) are considered to be the most important.

The present work in inviscid flow must be supplemented by comprehensive wind tunnel experiments to establish the nature and magnitude of viscous effects on swept wings with flaps and tip controls.

LIST OF SYMBOLS

x, y, z	Rectangular co-ordinates: x in the stream direction, $x = 0$ at the leading edge: y in the spanwise direction, positive to starboard: z positive downwards. x,y,z are non-dimensional in terms of the chord
x_v, y_v	Co-ordinates of the point of origin of a trailing vortex
x_H	x-co-ordinate of flap hinge
θ	Spanwise co-ordinate
η	Spanwise co-ordinate $= \dfrac{yc}{b/2}$ } $\theta = \cos^{-1}\eta$
θ_F	Spanwise co-ordinate of end of flap: $\theta_F = \cos^{-1}\eta_F$
η_F	
v_z	Induced velocity in vertical direction
v_{zm}	Mean value of v_z over the chord
$v_{z\infty}$	Value of v_z at infinity downstream
ω	Downwash factor
ω_1	Downwash factor on an unswept wing
ω_2	Downwash factor due to sweep
α	Geometric incidence
α_{i0}	Half induced incidence at infinity downstream
α_i	Induced incidence $= \omega\alpha_{i0}$
α_e	Effective incidence $= \alpha - \alpha_i$
γ	Non-dimensional vorticity
γ_I	Vorticity associated with a discontinuous incidence distribution
γ_{II}	$\gamma - \gamma_I$
a	Local lift slope $= \dfrac{C_L}{\alpha_e}$
a_0	Two-dimensional lift slope
b	Wing span
c	Chord (the unit of linear measurement)
c_F	Flap chord
n	Chordwise loading parameter
A	Aspect ratio
b_{vv}, b_{vn}	Multhopp coefficients
C_L	Local lift coefficient
$\overline{C_L}$	Overall lift coefficient
$\overline{C_l}$	Overall rolling moment coefficient
M_o	Free stream Mach number
$\Delta\alpha$	Equivalent incidence due to flap deflection
β	Angle of deflection of flap

σ	Discontinuity in incidence at end of flap
λ	Fading-out function for centre and tip effects
$\tau(\eta)$	Spanwise loading factor
φ	Angle of sweep, positive for sweepback
v	Suffix denoting spanwise pivotal point

REFERENCES

No.	*Author*	*Title, etc.*
1	H. Glauert	Theoretical relationships for an aerofoil with hinged flap A.R.C. R. & M. 1095, April, 1927.
2	F. Keune	*Auftrieb einer geknickten ebenen Platte.* Luftfahrtforschung, Vol. 13, p. 85, 1936.
3	F. Keune	*Momente und Ruderauftrieb einer geknickten ebenen Platte.* Luftfahrtforschung, Vol. 14, p. 558, 1937.
4	H. Multhopp	*Die Berechnung der Auftriebsverteilung von Tragflugeln.* Luftfahrtforschung, Vol. 15, p. 153, 1938. Translated in A.R.C. 8516.
5	H. Multhopp	Methods for calculating the lift distribution of wings (subsonic lifting surface theory). A.R.C. R. & M. 2884. Jan. 1950.
6	D. Küchemann	A simple method for calculating the span and chordwise loadings on straight and swept wings of any given aspect ratio at subsonic speeds. A.R.C. R. & M. 2935. August, 1952.
7	G. G. Brebner	The application of camber and twist to swept wings in incompressible flow. A.R.C. C.P. No. 171. March, 1952.
8	R. Duquenne and C. Grandjean	Calcul d'effets de volets par analogie rheoelectrique. ONERA Proces verbal d'essais No. 11/1292A, July 1954.
9	L. Malavard..	The use of rheo-electrical analogies in certain aerodynamical problems. *J.Roy. Aero. Soc.*, Vol. 51, p. 739, 1947.
10	J. Weber	Theoretical load distribution on a wing with vertical plates. A.R.C. R. & M. 2960. March, 1954.
11	L. Malavard and R. Duquenne	Etude des surfaces portantes par analogies rheoelectriques. *La Recherche Aeronautique*, No. 23, 1951. Translated in A.R.C. 15108.

REFERENCES—*continued*

No.	*Author*	*Title, etc.*
12	R. Duquenne	Application de l'analogie rheoelectrique au calcul de trois ailes de meme forme en plan. ONERA Note Technique 9/1292A, Sept. 1953.
13	H. H. B. M. Thomas and K. W. Mangler	All-moving wing tip controls at subsonic, sonic and supersonic speeds. A discussion of available theoretical methods and their application to a delta wing with half-delta controls. R.A.E. Report No. Aero 2499. A.R.C. 16274. July, 1953.
14	J. Weber and J. A. Lawford	The reflection effect of fences at low speeds. A.R.C. R. & M. 2977. May, 1954.
15	R. T. Jones	Properties of low-aspect-ratio pointed wings at speeds below and above the speed of sound. N.A.C.A. Report No. 835, 1946.
16	J. DeYoung	Theoretical symmetric span loading due to flap deflection for wings of arbitrary planform at subsonic speeds. N.A.C.A. Report, 1071, 1952.
17	J. DeYoung	Theoretical antisymmetric span loading for wings of arbitrary planform at subsonic speeds. N.A.C.A. Report 1056, 1951.
18	D. Küchemann	The distribution of lift over the surface of swept wings. Aeronaut Quart., Vol. IV., pp. 261–278. August, 1953.

APPENDIX I

The Downwash Factors, ω_1 and ω_2

Consider the constant-chord swept wing of Fig. 1. Let O be the origin of the co-ordinates (X, Y): $X = x + y \tan \varphi$, $Y = y$, and so $x = 0$ at the leading edge of the wing. All co-ordinates are non-dimensional in terms of the chord. Let AB be an isolated line vortex of strength $\dot{\gamma}$ in the free stream direction, extending from A (x_v, y_v) to infinity downstream. Then the downwash induced at $P(x,y)$ by this vortex is

$$v_z = \frac{\gamma}{4\pi(y-y_v)}(1+\cos\psi)$$

$$= \frac{\gamma}{4\pi(y-y_v)}\left(1-\frac{x_v+y_v\tan\varphi-x}{\sqrt{(x_v+y_v\tan\varphi-x)^2+(y-y_v)^2}}\right)$$

The mean value of v_z over the chord through P is therefore

$$v_{zm} = \frac{\gamma}{4\pi(y-y_v)}\int_{y\tan\varphi}^{y\tan\varphi+1}\left(1-\frac{x_v+y_v\tan\varphi-x}{\sqrt{(x_v+y_v\tan\varphi-x)^2+(y-y_v)^2}}\right)dX$$

$$= \frac{\gamma}{4\pi(y-y_v)}\left(1+\sqrt{[x_v-1-(y-y_v)\tan\varphi]^2+(y-y_v)^2}\right.$$

$$\left.-\sqrt{[x_v-(y-y_v)\tan\varphi]^2+(y-y_v)^2)}\right)$$

When $\varphi = 0°$,

$$[v_{zm}]_{0°} = \frac{\gamma}{4\pi(y-y_v)}\left(1+\sqrt{(x_v-1)^2+(y-y_v)^2}\right.$$

$$\left.-\sqrt{x_v^2+(y-y_v)^2}\right)$$

Half the downwash at infinity downstream is

$$\frac{v_{z\infty}}{2} = \frac{\gamma}{4\pi(y-y_v)}$$

and the downwash factor for unswept wings, ω_1 is

$$\omega_1 = \frac{[v_{zm}]_{0°}}{\frac{1}{2}v_{z\infty}}$$

$$= 1+\sqrt{(x_v-1)^2+(y-y_v)^2}-\sqrt{x_v^2+(y-y_v)^2}$$

ω_1 is plotted against $|y-y_v|$ in Fig. 2 for various values of x_v.

As $|y-y_v| \to \infty$ we can write

$$\omega_1 = 1+(y-y_v)\sqrt{\frac{(x_v-1)^2}{(y-y_v)^2}+1}-(y-y_v)\sqrt{\frac{x_v^2}{(y-y_v)^2}+1}$$

$$= 1+(y-y_v)\left\{1+\tfrac{1}{2}.\frac{(x_v-1)^2}{(y-y_v)^2}+\ldots\right\}$$

$$-(y-y_v)\left\{1+\tfrac{1}{2}.\frac{x_v^2}{(y-y_v)^2}+\ldots\right\}$$

$$\to 1 \text{ as } |y-y_v| \to \infty$$

The downwash factor due to sweep, ω_2 is

$$\omega_2 = \frac{[v_{zm}]_\varphi}{[v_{zm}]_{0^0}}$$

$$= \frac{1+\sqrt{[x_v-1-(y-y_v)\tan\varphi]^2+(y-y_v)^2}-\sqrt{[x_v-(y-y_v)\tan\varphi]^2+(y-y_v)^2}}{1+\sqrt{(x_v-1)^2+(y-y_v)^2}-\sqrt{x_v^2+(y-y_v)^2}}$$

ω_2 is plotted against $y-y_v$ in Fig. 3 for various values of x_v.

$$\omega_2 > 1 \text{ for } \left.\begin{matrix} y-y_v>0 \\ \varphi>0 \end{matrix}\right\} \text{: or } \left.\begin{matrix} y-y_v<0 \\ \varphi<0 \end{matrix}\right\}$$

$$\omega_2 < 1 \text{ for } \left.\begin{matrix} y-y_v<0 \\ \varphi>0 \end{matrix}\right\} \text{: or } \left.\begin{matrix} y-y_v>0 \\ \varphi<0 \end{matrix}\right\}$$

As $y-y_v \to +\infty$ we can write

$$\omega_2 = 1+\sqrt{(y-y_v)^2(1+\tan^2\varphi)+(x_v-1)^2-2(x_v-1)(y-y_v)\tan\varphi}$$
$$-\sqrt{(y-y_v)^2(1+\tan^2\varphi)+x_v^2-2x_v(y-y_v)\tan\varphi}$$

$$= 1+(y-y_v)\sqrt{1+\tan^2\varphi}\left\{\sqrt{1+\frac{(x_v-1)^2}{(y-y_v)^2(1+\tan^2\varphi)}-\frac{2(x_v-1)\tan\varphi}{(y-y_v)(1+\tan^2\varphi)}}\right.$$

$$\left.-\sqrt{1+\frac{x_v^2}{(y-y_v)^2(1+\tan^2\varphi)}-\frac{2x_v\tan\varphi}{(y-y_v)(1+\tan^2\varphi)}}\right\}$$

$$= 1+(y-y_v)\sqrt{1+\tan^2\varphi}\left\{1+\tfrac{1}{2}\left[\frac{(x_v-1)^2}{(y-y_v)^2(1+\tan^2\varphi)}-\frac{2(x_v-1)\tan\varphi}{(y-y_v)(1+\tan^2\varphi)}\right]\right.$$

$$+\ldots\ldots$$

$$\left.-1-\tfrac{1}{2}\left[\frac{x_v^2}{(y-y_v)^2(1+\tan^2\varphi)}-\frac{2x_v\tan\varphi}{(y-y_v)(1+\tan^2\varphi)}\right]-\ldots\ldots\right\}$$

$$\rightarrow 1+\sqrt{1+\tan^2\varphi}\cdot\frac{\tan\varphi}{1+\tan^2\varphi}$$

$$=1+\sin\varphi \text{ as } y-y_v\rightarrow+\infty$$

Similarly $\omega_2\rightarrow 1-\sin\varphi$ as $y-y_v\rightarrow-\infty$.

APPENDIX II

Multhopp's Spanwise Loading Function, γ_I, for Unswept Wings

Let σ be the discontinuous change of incidence at the end of the flap,

$$\theta = \cos^{-1}\eta$$

$$\theta_F = \cos^{-1}\eta_F$$

(i) Outboard flaps: symmetrically deflected:

$$\gamma_I(\theta)=\frac{2\sigma}{\pi}\left[(\cos\theta-\cos\theta_F)\,ln\frac{\sin\frac{\theta+\theta_F}{2}}{\sin\frac{|\theta-\theta_F|}{2}}+\right.$$

$$\left.+(\cos\theta-\cos\theta_F)\,ln\frac{\cos\frac{\theta+\theta_F}{2}}{\cos\frac{\theta-\theta_F}{2}}+2\theta_F\sin\theta\right]$$

(ii) Outboard flaps; antisymmetrically deflected:

$$\gamma_I(\theta)=\frac{2\sigma}{\pi}\left[(\cos\theta-\cos\theta_F)\,ln\frac{\sin\frac{\theta+\theta_F}{2}}{\sin\frac{|\theta-\theta_F|}{2}}-\right.$$

$$\left.-(\cos\theta+\cos\theta_F)\,ln\frac{\cos\frac{\theta+\theta_F}{2}}{\cos\frac{\theta-\theta_F}{2}}\right]$$

(iii) Inboard flaps: symmetrically deflected:

$$\gamma_I(\theta) = \frac{2\sigma}{\pi}\left[(\pi - 2\theta_F)\sin\theta - (\cos\theta - \cos\theta_F)\ln\frac{\sin\frac{\theta+\theta_F}{2}}{\sin\frac{|\theta-\theta_F|}{2}}\right.$$

$$\left. -(\cos\theta + \cos\theta_F)\ln\frac{\cos\frac{\theta+\theta_F}{2}}{\cos\frac{\theta-\theta_F}{2}}\right]$$

TABLE I

Spanwise Loading Factor, $\tau(\eta)$: $\varphi = 45$ deg Symmetrical Deflection

	Inboard Flaps				Outboard Flaps			
η \ η_F	0·25	0·45	0·65	0·85	0·25	0·45	0·65	0·85
		$x_H = 0{\cdot}65$				$x_H = 0{\cdot}65$		
0	1·394	1·298	1·225	1·169	0·937	0·825	0·751	0·619
0·195	1·440	1·311	1·231	1·168	0·937	0·814	0·720	0·604
0·383	1·646	1·355	1·248	1·172	0·960	0·838	0·728	0·580
0·556	1·742	1·508	1·282	1·185	0·991	0·879	0·747	0·570
0·707	1·776	1·563	1·373	1·193	1·009	0·913	0·814	0·586
0·832	1·766	1·596	1·410	1·212	1·006	0·918	0·839	0·637
0·924	1·752	1·601	1·408	1·263	0·987	0·913	0·839	0·729
0·981	1·785	1·591	1·423	1·286	0·985	0·920	0·848	0·729
		$x_H = 0{\cdot}75$				$x_H = 0{\cdot}75$		
0	1·461	1·330	1·244	1·190	0·861	0·741	0·617	0·300
0·195	1·512	1·341	1·251	1·191	0·873	0·751	0·611	0·293
0·383	1·738	1·395	1·263	1·195	0·918	0·770	0·633	0·292
0·556	1·829	1·547	1·303	1·204	0·960	0·851	0·677	0·338
0·707	1·860	1·611	1·395	1·218	0·984	0·892	0·792	0·440
0·832	1·870	1·644	1·440	1·242	0·980	0·903	0·809	0·567
0·924	1·851	1·673	1·429	1·297	0·964	0·895	0·819	0·686
0·981	1·869	1·671	1·453	1·309	0·959	0·884	0·800	0·702
		$x_H = 0{\cdot}85$				$x_H = 0{\cdot}85$		
0	1·551	1·353	1·276	1·205	0·805	0·722	0·558	0·184
0·195	1·617	1·366	1·280	1·205	0·816	0·728	0·545	0·179
0·383	1·822	1·427	1·298	1·210	0·887	0·731	0·550	0·191
0·556	1·932	1·576	1·358	1·220	0·931	0·833	0·575	0·225
0·707	1·990	1·633	1·483	1·231	0·945	0·871	0·726	0·273
0·832	2·002	1·669	1·511	1·265	0·948	0·881	0·779	0·411
0·924	2·017	1·710	1·516	1·303	0·936	0·876	0·796	0·671
0·981	2·061	1·698	1·522	1·316	0·936	0·864	0·778	0·688

TABLE 2

Overall lift and rolling moment of delta wing with all-moving tips

	η_F	$\bar{C}_L/\beta$			$\bar{C}_l/\beta$		
		Ref. 13		Present method (a) $A = 1{\cdot}848$	Ref. 13		Present method (a) $A = 1{\cdot}848$
		(c) Multhopp Fairing	(d) Unfaired		(c) Multhopp Fairing	(d) Unfaired	
symmetric deflection	0·67	0·3661	0·4126	0·41	—	—	—
	0·74	0·2391	0·1799	0·28	—	—	—
Antisymmetric deflection	0·67	—	—	—	0·0967	0·1077	0·111
	0·74	—	—	—	0·0680	0·0542	0·080

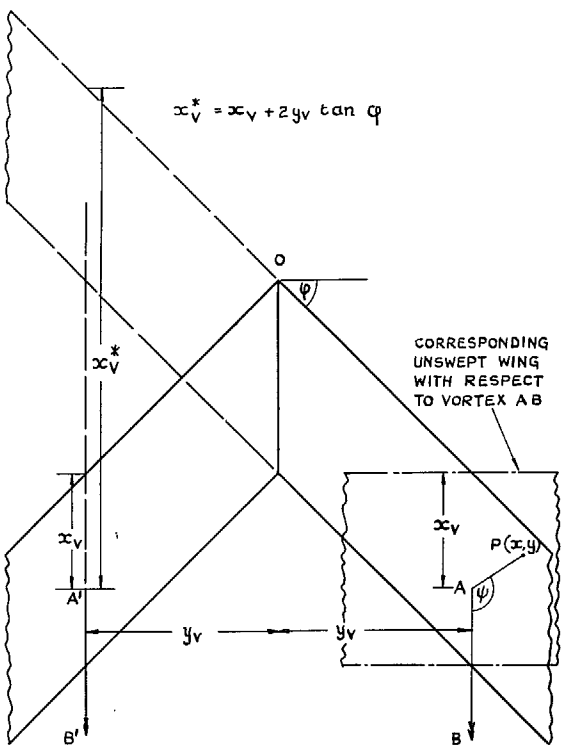

FIG. 1. Co-ordinate system of trailing vortices on swept and unswept wings.

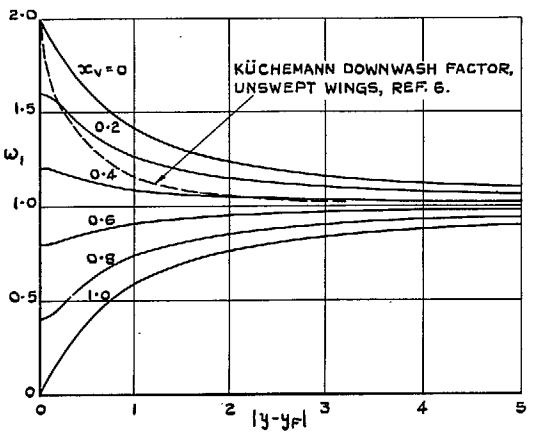

FIG. 2. Downwash Factor, ω_1.

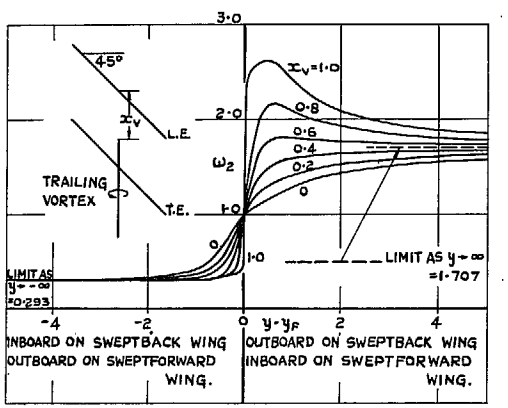

FIG. 3. Downwash factor, ω_2.

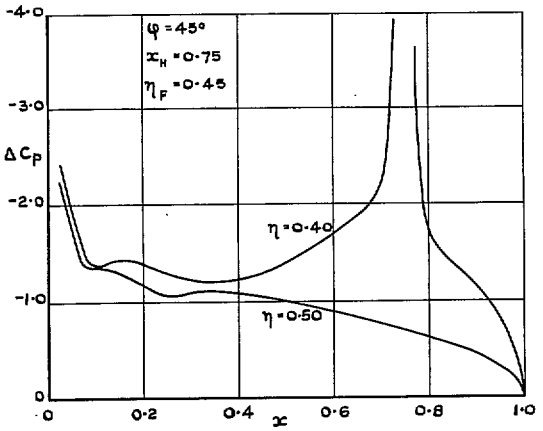

FIG. 4. Typical Chordwise loadings: Electric tank results.

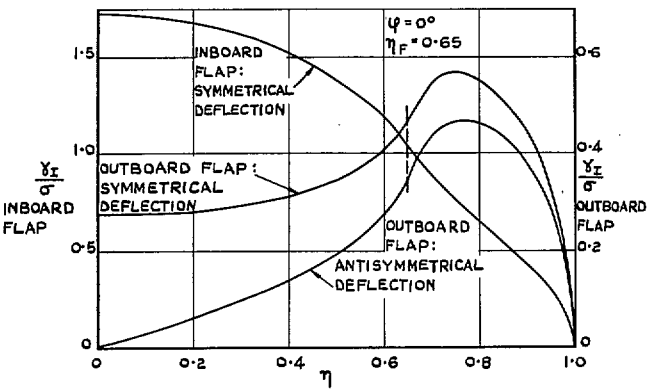

FIG. 5. Some typical Multhopp spanwise loading functions for discontinuous incidence.

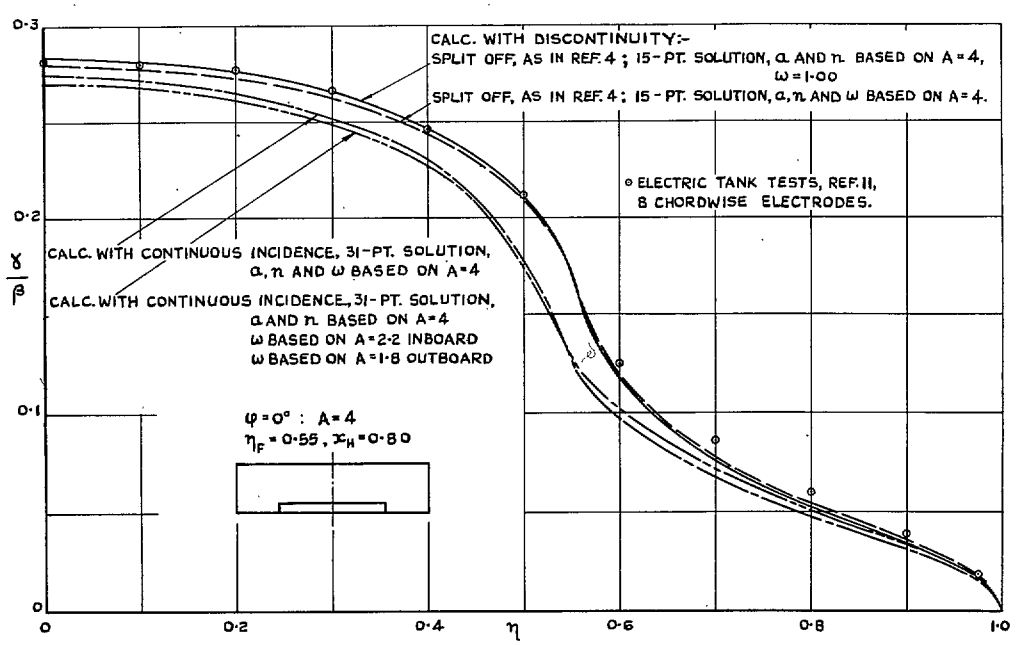

FIG. 6. Spanwise loading of an unswept wing with inboard flap.

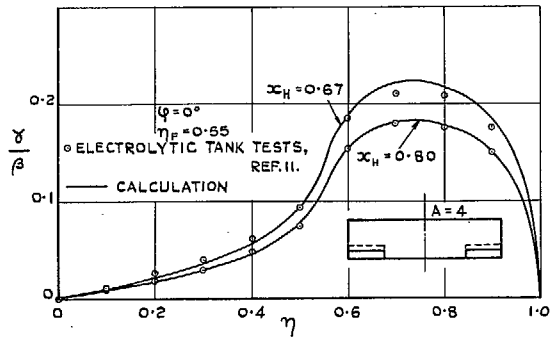

FIG. 7. Spanwise loading of an unswept wing with outboard flap.

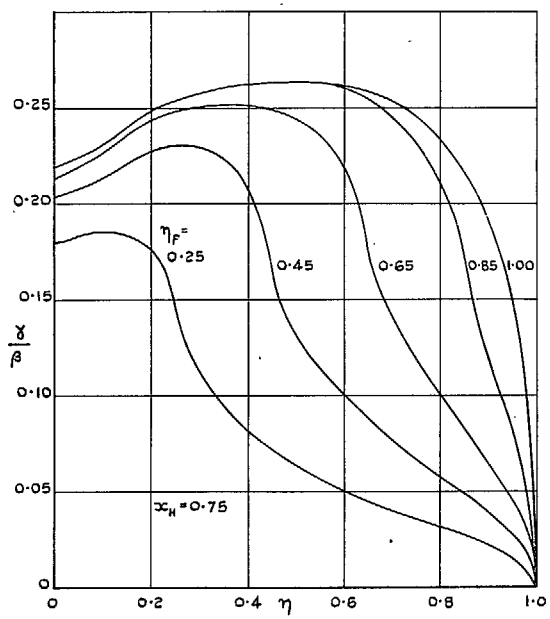

FIG. 8. Typical spanwise loadings of a 45 deg sweptback wing with flaps: electric tank results.

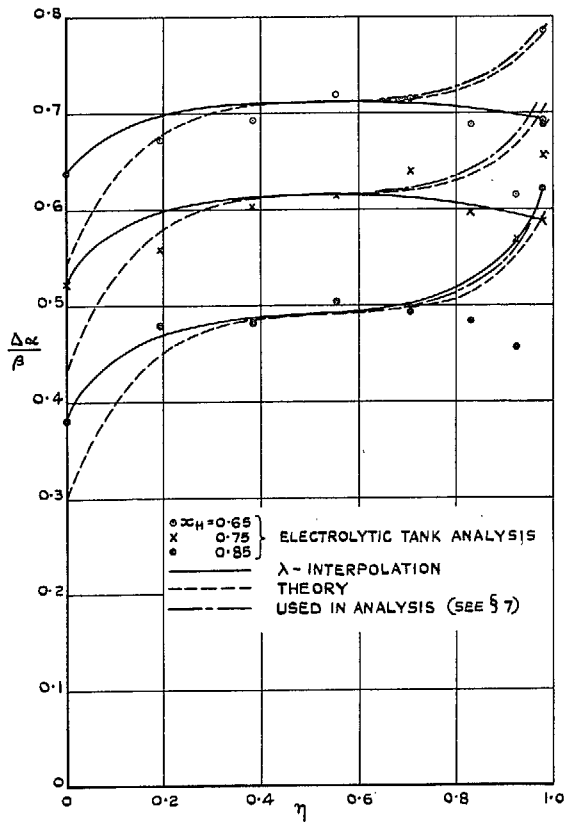

FIG. 9. Spanwise variation of equivalent incidence.

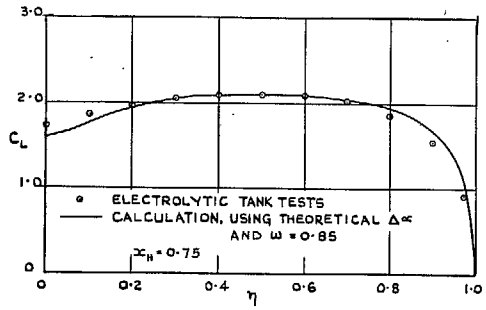

FIG. 10. Spanwise loading of a 45 deg sweptback wing with full-span flap.

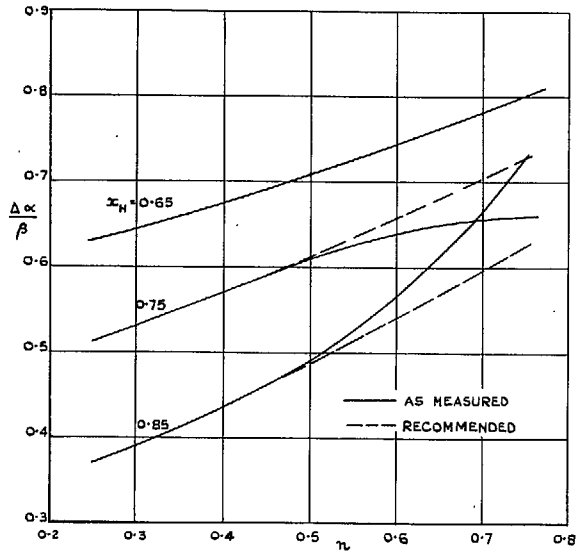

FIG. 11. Variation of equivalent incidence with (η).

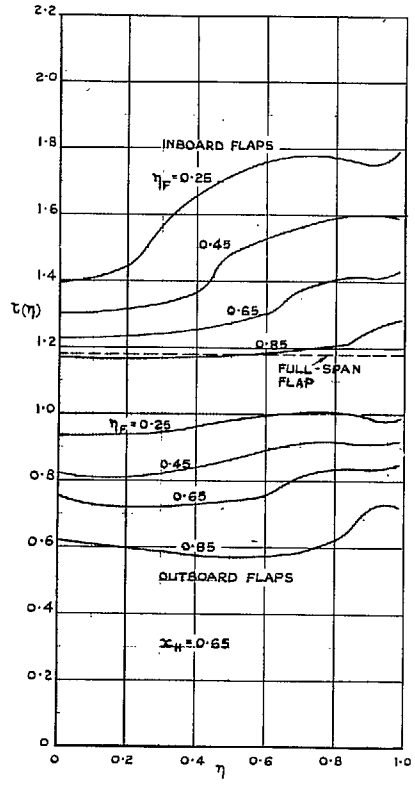

FIG. 12. Spanwise loading factor, $\tau(\eta)$: $x_H = 0{\cdot}65$.

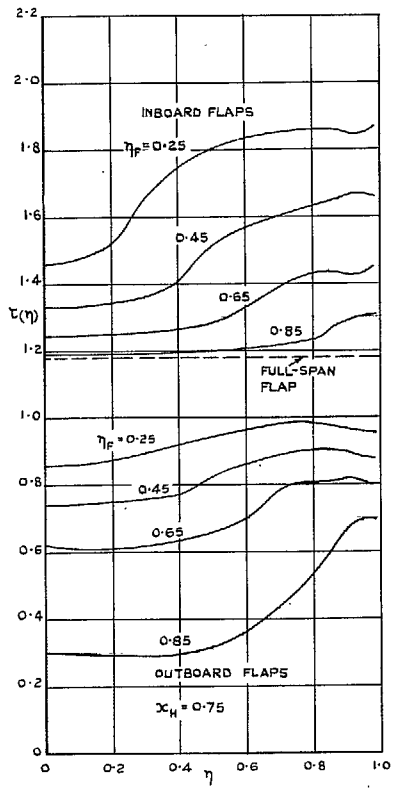

FIG. 13. Spanwise loading factor, $\tau(\eta)$: $x_H = 0{\cdot}75$.

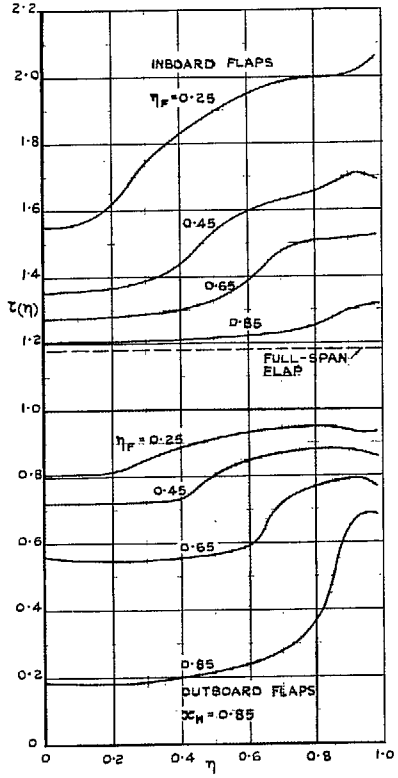

FIG. 14. Spanwise loading factor, $\tau(\eta)$: $x_H = 0{\cdot}85$.

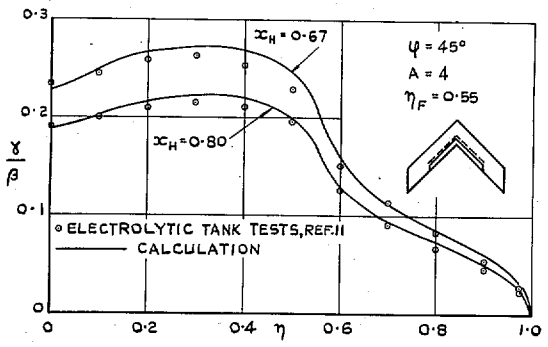

FIG. 15. Spanwise loading of a 45 deg sweptback wing with inboard flaps.

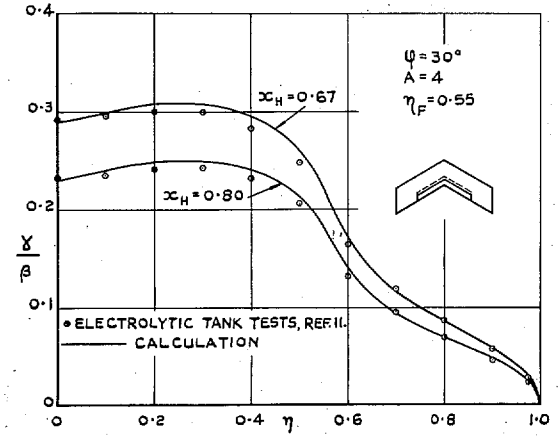

FIG. 16. Spanwise loading of a 30 deg sweptback wing with inboard flaps.

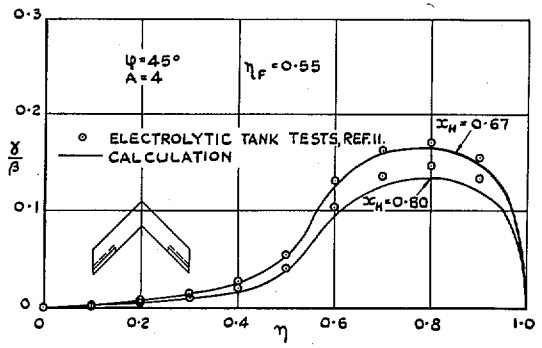

FIG. 17. Spanwise loading of a 45 deg sweptback wing with outboard flaps, anti-symmetrically deflected.

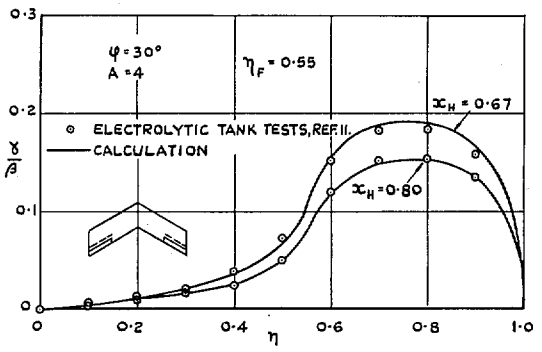

FIG. 18. Spanwise loading of a 30 deg sweptback wing with outboard flaps, anti-symmetrically deflected.

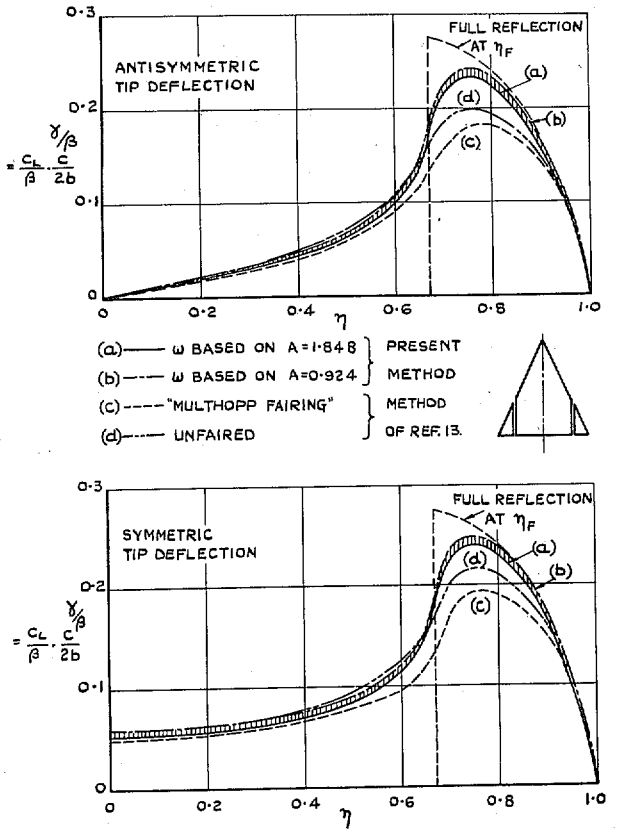

FIG. 19. Spanwise loadings of a delta wing with all-moving tip: $A = 1{\cdot}848$, $\eta_F = 0{\cdot}67$.

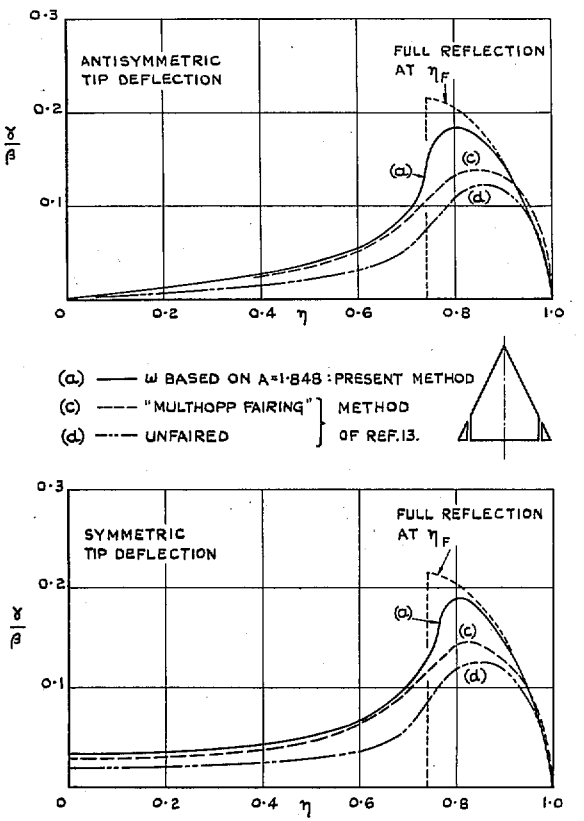

FIG. 20. Spanwise loadings of a delta wing with all-moving tip. $A = 1{\cdot}848$; $\eta_F = 0{\cdot}74$.

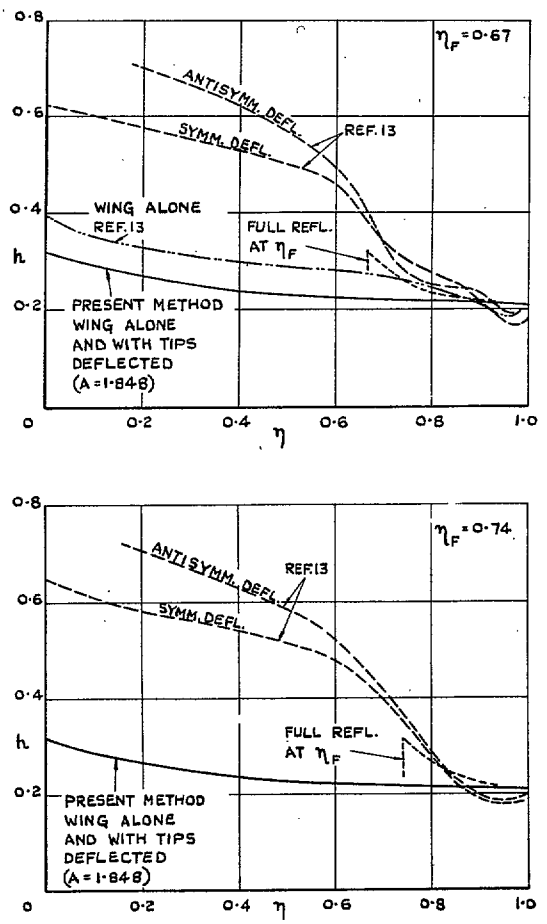

FIG. 21. Spanwise variation of the local aerodynamic centre for a delta wing with all-moving tip. $A = 1·848$.

Printed in Wales for Her Majesty's Stationery Office by Allens, Printers (Wales), Limited

D.125874 K.5

Published by
HER MAJESTY'S STATIONERY OFFICE

To be purchased from
49 High Holborn, London W.C.1
423 Oxford Street, London W.1
13A Castle Street, Edinburgh 2
109 St. Mary Street, Cardiff
Brazennose Street, Manchester 2
50 Fairfax Street, Bristol 1
35 Smallbrook, Ringway, Birmingham 5
7–11 Linenhall Street, Belfast 2
or through any bookseller

S.O. Code No. 23–3487